NREL
NATIONAL RENEWABLE ENERGY LABORATORY

Algorithm for Screening Phasor Measurement Unit Data for Power System Events and Categories and Common Characteristics for Events Seen in Phasor Measurement Unit Relative Phase-Angle Differences and Frequency Signals

A. Allen
National Renewable Energy Laboratory

S. Santoso
University of Texas at Austin

E. Muljadi
National Renewable Energy Laboratory

NREL is a national laboratory of the U.S. Department of Energy
Office of Energy Efficiency & Renewable Energy
Operated by the Alliance for Sustainable Energy, LLC

This report is available at no cost from the National Renewable Energy Laboratory (NREL) at www.nrel.gov/publications.

Technical Report
NREL/TP-5500-58611
August 2013

Contract No. DE-AC36-08GO28308

NREL
NATIONAL RENEWABLE ENERGY LABORATORY

Algorithm for Screening Phasor Measurement Unit Data for Power System Events and Categories and Common Characteristics for Events Seen in Phasor Measurement Unit Relative Phase-Angle Differences and Frequency Signals

A. Allen
National Renewable Energy Laboratory

S. Santoso
University of Texas at Austin

E. Muljadi
National Renewable Energy Laboratory

Prepared under Task No. WE11.0825

NREL is a national laboratory of the U.S. Department of Energy
Office of Energy Efficiency & Renewable Energy
Operated by the Alliance for Sustainable Energy, LLC

This report is available at no cost from the National Renewable Energy Laboratory (NREL) at www.nrel.gov/publications.

National Renewable Energy Laboratory
15013 Denver West Parkway
Golden, CO 80401
303-275-3000 • www.nrel.gov

Technical Report
NREL/TP-5500-58611
August 2013

Contract No. DE-AC36-08GO28308

This report is available at no cost from the National Renewable Energy Laboratory (NREL) at www.nrel.gov/publications.

Available electronically at http://www.osti.gov/bridge

Available for a processing fee to U.S. Department of Energy and its contractors, in paper, from:

U.S. Department of Energy
Office of Scientific and Technical Information
P.O. Box 62
Oak Ridge, TN 37831-0062
phone: 865.576.8401
fax: 865.576.5728
email: mailto:reports@adonis.osti.gov

Available for sale to the public, in paper, from:

U.S. Department of Commerce
National Technical Information Service
5285 Port Royal Road
Springfield, VA 22161
phone: 800.553.6847
fax: 703.605.6900
email: orders@ntis.fedworld.gov
online ordering: http://www.ntis.gov/help/ordermethods.aspx

Cover Photos: (left to right) photo by Pat Corkery, NREL 16416, photo from SunEdison, NREL 17423, photo by Pat Corkery, NREL 16560, photo by Dennis Schroeder, NREL 17613, photo by Dean Armstrong, NREL 17436, photo by Pat Corkery, NREL 17721.

Printed on paper containing at least 50% wastepaper, including 10% post consumer waste.

Acknowledgments

The authors acknowledge Dr. Mack Grady for his guidance during the development of this project. Doctors Wei-Jen Lee of the University of Texas at Arlington and Jamie Ramos of the University of Texas–Pan American provided a thorough review of this report and insightful comments and suggestions. We also acknowledge National Renewable Energy Laboratory colleagues Yih-Huei Wan, Yingchen Zhang, Vahan Gevorgian, and Mohit Singh, who supported this effort in many different capacities.

List of Acronyms

CSV	comma-separated value
ERCOT	Electric Reliability Council of Texas
FFT	fast Fourier transform
PMU	phasor measurement unit
PSD	power spectral density
RPAD	relative phase angle difference
UT-Austin	University of Texas at Austin
UTC	Coordinated Universal Time
UTPA	University of Texas–Pan American

Executive Summary

A network of multiple phasor measurement units (PMU) was created, set up, and maintained by professors and students from the University of Texas at Austin to obtain actual power system measurements for power system analysis. The network is now located and maintained at Baylor University in Waco, Texas. Power system analysis in this report covers a variety of time ranges, such as short-term analysis for power system disturbances and their effects on power system behavior and long-term power system behavior using modal analysis. Modal analysis is the analysis of power system dynamic behavior under excitation from changes in the power system. The PMU data examined in this report is archived at 30 samples per second and is continuously measuring and recording voltage phasor data. Because of the high volume of PMU data generated by the network, it is difficult to localize and analyze power system abnormal events (large disturbance events) of interest that have been recorded by the network.

The first objective of this report is to screen the PMU data for events. An algorithm was created using a variety of methods to detect power system events. The algorithm uses fast Fourier transform-, Yule-Walker-, and matrix-pencil-based methods to find events as well as a simple method to detect large swings in the PMU data.

The second objective of the report is to identify and describe common characteristics extracted from power system events as measured by PMUs. The report describes category definitions based on visual analysis and extraction of numerical characteristics for each category. Category definitions based on visual inspection consist of two parts: events detected in voltage phase angle signals and frequency signals. In the voltage phase angle, events belong to one or more of the following proposed categories: impulse, transient, or step change. In the frequency, events belong to one or more of the following proposed categories: impulse, transient, or rise or drop in frequency. Some events belong to one category; some events belong to multiple categories, such as frequency drops caused by a sudden loss of generation that can also contain low-frequency oscillations. This type of event belongs to both the drop-in-frequency and transient categories.

The numerical characteristics for each category and how these characteristics are used to create selection rules for the algorithm are also described. Trends in PMU data related to different levels and fluctuations in wind power output are also examined.

Table of Contents

List of Figures

List of Tables

1 Introduction (and Background)

Wide-area monitoring systems based on phasor measurement units (PMUs) collect large amounts of power system data in the form of phasors. Wide-area monitoring systems are intended for use across large geographical areas. With these actual power system measurements, it is possible to identify system trends and behavior such as power system frequency and voltage phase angle responses to factors such as increasing load or increasing penetrations of renewable energy resources. PMUs generate high precision data typically at a rate of 30 observations per second, resulting in large volumes of phasor data. In larger wide-area monitoring systems containing a large number of PMUs, the amount of data generated can be difficult to handle. Eventually, PMU data and wide-area monitoring systems can be used to help power system operators make better-informed decisions to keep the power system stable and operational. However, before this can occur, power system behavior as seen through PMU data must be understood.

The purpose of the research presented herein is to better understand power system behavior by detecting power system events of importance and also to begin examining trends and the behavior of the power system under different operating conditions. Algorithms are created to screen the large volumes of PMU data for power system events. The algorithms are applied to many days of PMU data so that many events are detected during different operating conditions (different times of the day and different seasons) and at different locations within the PMU network. These events are analyzed and placed into categories based on similar visual characteristics. The research presented here also describes common quantitative characteristics in each event category and the ranges of characteristics for each event category. Eventually, conditions before and after each event type will be examined to determine which event categories could cause changes in power system behavior.

In the future, power system operators will be alerted through real time detection of harmful events that are occurring and/or incoming on the system. The stability margin will be gauged more accurately, and possible remedial actions could be prescribed ahead of time.

All data used in this research are real power system measurements taken from PMUs. The following sections describe the PMU network and data, screening algorithms to detect power system events in the data, and categorization of events based on common characteristics.

1.1 Independent Synchrophasor Network and PMU Data

Synchronized voltage measurements taken by PMUs allow for wide-area monitoring of the electric power system. However, the placement of PMUs and use of PMU data are generally controlled by utilities and the independent system operators that install them. Data are not always readily available for research. To overcome this obstacle, the University of Texas at Austin (UT-Austin) introduced an independent synchrophasor network to monitor events and analyze low-frequency oscillations from the electric power grid through PMU measurements taken at the customer-level voltage (120 V).

PMUs can now be placed virtually anywhere throughout the electric power system, and measurements are freely available to use for power system analysis. A map of the locations of the Independent Texas Synchrophasor Network PMUs within the Electric Reliability Council of Texas (ERCOT) is shown in Figure 1. PMU stations were placed within different zones of ERCOT: the Waco PMU station is located in the North Zone; the UT-Pan American and UT-Austin PMU stations are located in the South Zone; the Schweitzer Engineering Laboratories, Inc. (SEL) – Houston PMU station is located in the Houston Zone; and the McDonald Observatory PMU station is located in the West Zone. The McDonald Observatory PMU location was selected also because of its proximity to wind farms in West Texas, as shown in Figure 2. Information on transmission level power system event and behavior is clearly captured by 120 V PMUs as shown in [1].

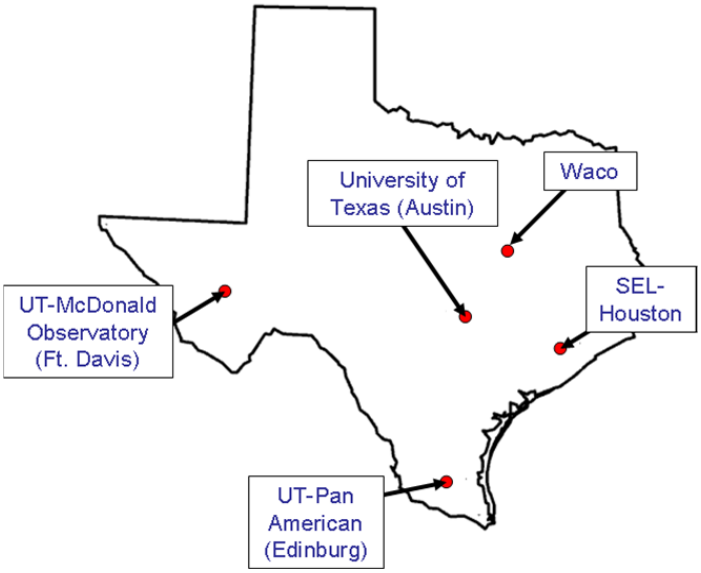

Figure 1. Map of Texas PMU stations within the UT-Austin Independent Texas Synchrophasor Network

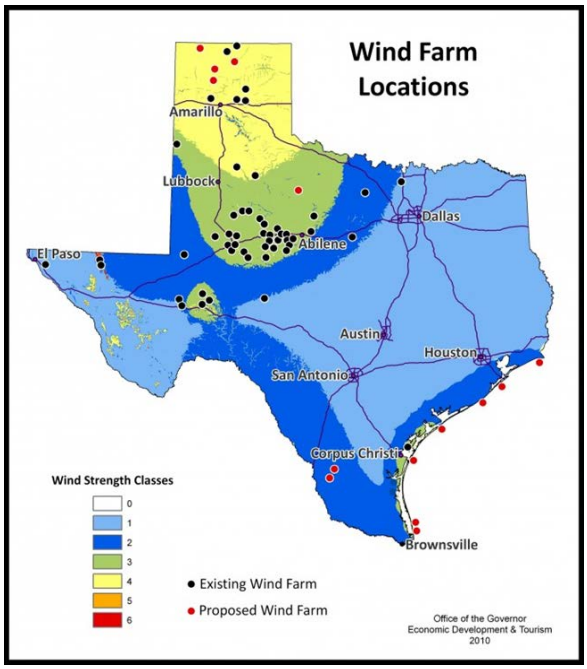

Figure 2. Map of wind farm locations in Texas [2]

A diagram of equipment at each PMU location and central phasor data concentrator within the synchrophasor network is shown in Figure 3. All equipment was donated by Schweitzer Engineering Laboratories, Inc. As shown in Figure 3, each PMU station has an antenna to receive a global positioning system signal. This global positioning system signal is the common time reference required to make synchronous phasor measurements. The global positioning system signal is sent to the global positioning system receiver, where it is converted to Coordinated Universal Time (UTC) and used by each PMU to time stamp the measured phasor quantity. The time-stamped phasor from each PMU station is sent either through public internet or serial cable to the phasor data concentrator. The phasor data concentrator waits for data from all PMU locations and sorts the PMU data once it is received. The collected data is sent to a dedicated desktop PC, where software provided by Schweitzer Engineering Laboratories, Inc., archives the PMU data and displays it in real time.

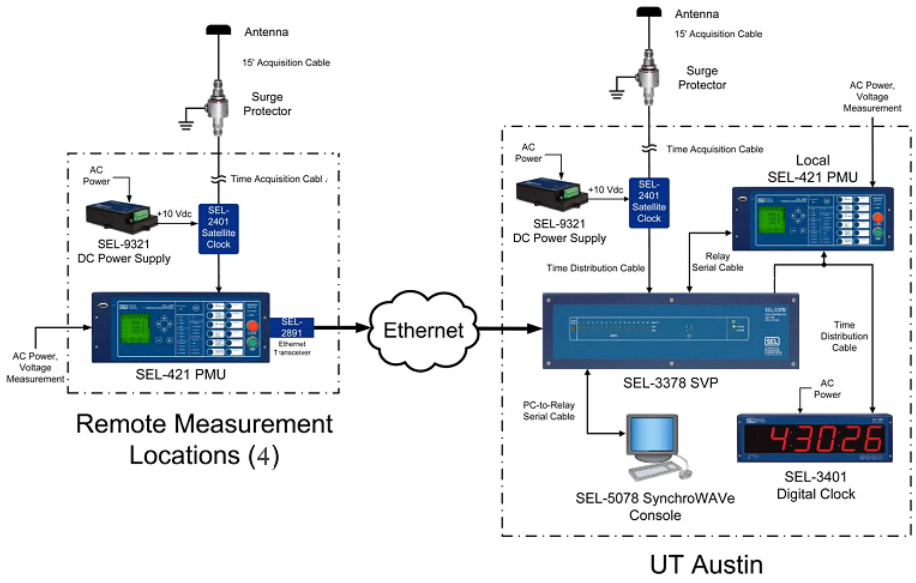

Figure 3. (Left) Equipment for each PMU station and (right) the phasor data concentrator and PC within the Independent Texas Synchrophasor Network

The synchronized phasor measurements and calculated frequency are stored at a rate of 30 data points per second. Because the data has a 30-Hz sampling rate, only low-frequency oscillations (below 15 Hz) can be analyzed. Events such as capacitor bank switching, which induces oscillations on the order of a few hundreds of hertz to 1.5 kHz, are not visible in the PMU data. Even with a sampling rate of 30 Hz, the archived hourly reports are very large. For one PMU, an hourly report of the voltage phase angle data consists of 108,000 data points. Because there are three signals for each PMU station (voltage phase angle, voltage magnitude, and frequency), each PMU station generates 324,000 data points each hour. These data points are stored hourly in a comma-separated value (CSV) format. A network with five PMU stations generates hourly CSV reports that are 13.8 MB in size. The synchrophasor network is in operation at all times.

Since the network was set up in the fall of 2008, it has been continuously generating data. Because so much data is being generated, it is difficult to detect events of interest and analyze them for power system studies. Resources such as ERCOT's Daily Grid Operations Reports [3] provide information on sudden losses of power above 450 MW caused by generating unit trips and information on line contingencies. (Total peak generating capacity in ERCOT is above 65 GW.) In addition, it is generally straightforward to visually detect large, sudden imbalances in generation and load by monitoring frequency. However, information related to events such as transmission line reclosing and trips and other equipment trips is not readily available. The research presented herein examines if these system events are visible in the PMU data and if it is possible to automatically detect events of interest.

In this report, the voltage phase angle difference between two PMU locations is used to detect power system events that are visible in the voltage phase angle signal. However,

ideally when there are a large number of PMUs installed in the system, a common reference phase angle for all PMUs is desired. This reference phase angle can be determined by using a center-of-gravity concept to PMU-derived local frequencies. A common phase angle reference can then be subsequently obtained from this center-of-gravity frequency. Any PMUs located within the interconnected system can be referenced to this center-of-gravity derived reference frequency or reference phase angle. There are many power system measurements available to estimate center of gravity, as is well known in the literature [4] and will not be discussed here.

Data from five PMUs are available at five separate locations, with the distance between any two PMUs being very large. For example, the shortest geographical distance between two PMUs is approximately 105 miles; the closest two PMUs in the network are Waco and UT-Austin. The longest distance between two PMUs is between McDonald (Ft. Davis) and the University of Texas–Pan American (UTPA) (Edinburg); the geographical distance between these two PMUs is approximately 560 miles.

These PMUs are located among many generation buses (many of which are PV buses) that maintain the scheduled generation and scheduled bus voltage (V = 0.95 p.u. to 1.05 p.u.). The McDonald PMU is located among wind power plants that are operated as PQ buses (delivering power at specified real and reactive power; many wind plants are operated at unity power factor). When two PMUs are installed at buses located at opposite ends of a transmission line, the voltage phase angle difference and power transfer between the two adjacent buses can be measured and computed. However, when there are many generators and loads connected to the network between two PMUs at opposite ends of the power system network, the measured data between them cannot be used to directly measure the voltage phase angle difference or the power transfer.

The voltage phase angle difference between any two PMUs available in this project cannot be used to estimate the power transfer; instead, the PMUs are used to measure power system oscillations and other power system events. Two different PMU signals—voltage phase angle and frequency—are used to screen for power system events. As previously stated, because of limited numbers of PMUs installed in this area, the center-of-gravity concept is not applied; instead, the difference in phase angle between two PMUs (relative phase angle difference, RPAD) is used as a sensing variable to detect power system events. Note that the frequency is computed at each PMU.

Although the frequency is calculated by the PMU, different categories of events are visible in the frequency data that are not easily detected in the RPAD. Also, the frequency is taken from a single location requiring only a single PMU measurement; whereas the RPAD is actually the angle difference between two separate PMU locations. Some events that occur closer to one PMU location are stronger in the measured signal of that PMU, and therefore may be more easily detected in the frequency signal. The event in the measured RPAD signal may be drowned out by the voltage phase angle from the opposite PMU location. Also, the RPAD may reveal possible event sources that are not as obvious in the frequency signal. One possible drawback is the difficulty to diagnose and categorize events in case there are two independent events occurring at the same time at

two different locations. However, if this happens, other PMU signals can collectively help decipher the event.

1.2 Screening Algorithm

The term *event* in the report is used to describe large disturbances on the power system and sudden changes in power output at wind farms. Large disturbances include but are not limited to short circuits on transmission lines; protective relay actions required to clear the fault, such as transmission line trip and reclosing actions; or a large and sudden loss of generation or load. A sudden change in renewable energy includes but is not limited to large ramping up or down of wind farm power output. Large disturbances excite a single or multiple modes within the power system; these can be measured as oscillations in PMU voltage data. These oscillations typically consist of one strong mode in which the frequency of the oscillation is between 0.1 Hz and 2.0 Hz, the amplitude of the oscillation is typically higher than oscillations induced by random load switching, and the oscillation is quickly damped out if the system is stable. For example, a low-frequency oscillation of 0.3 Hz with a damping constant of 10% has a time constant of 5.3 seconds (the signal would drop to 37% of its original value after 5.3 seconds). This information is used to detect events in the PMU data. However, it is difficult to verify the cause of many of the detected events. The root cause of a few of the detected events can be identified; however, not all causes are known because information on power system disturbances is not always available or shared. Most of the guessed causes of events are based on clues present in the PMU data. Also, wind power-induced events are difficult to describe because detailed measurements of renewable generation power output is necessary for a thorough analysis.

The purpose of the PMU network is to conduct analysis on transmission system behavior, but because the measurements are taken at the customer-level voltage of 120 V, events on distribution system may be measured and recorded as well. However, the voltage magnitude at the customer level is more heavily impacted by events that occur on the distribution system. Also, large events that occur on the transmission system are visible at multiple PMU locations rather than at a single PMU location as is the case for distribution events. If it is unclear if a detected event occurred on the distribution system or the transmission system, the data from multiple PMUs can be compared during the time of the event and the voltage magnitude can be checked as well. If the event appears at only one PMU location and the voltage magnitude drops significantly (to 95% or less of rated voltage), then the event should not be considered a transmission system event. This type of event should be attributed to distribution system changes and should not be considered for transmission system analysis. Therefore, by using the guidelines above, it is important to distinguish between these two types of events so that distribution system events are not incorrectly identified and interpreted as transmission system events.

In Section 2, an algorithm to read PMU data from CSV data files is described as well as methods used to correct PMU data before analysis can begin. Section 2 also describes the algorithm implemented to screen PMU data for events. The algorithm includes multiple methods that analyze data for possible events and displays the detected events. Section 3 describes results of the application of the algorithm to PMU data and gives examples of

different types of events that were detected. For example, a large event visible at multiple PMUs is analyzed as well as smaller events visible at only one PMU location. Both the PMU measured voltage phase angle and PMU calculated frequencies are used to detect events.

1.3 Categorization of Power System Events

Events in the PMU RPAD and frequency signals detected by the screening algorithm are analyzed further. To extract common characteristics, the events detected by the screening algorithm are placed into event categories. Event categories are created for events detected in the RPAD signal and for events detected in the frequency signal. In Section 4, a description of how these categories are created based on common visual characteristics is provided. Examples of events in the voltage phase angle and frequency signals are provided and described in Section 4.1.1 and Section 4.1.2, respectively. These categories were selected after examining many events that occur at different times of the day, seasons, and are measured at different locations within the PMU network. A variety of methods are applied to the data to extract different characteristics from each group. The numerical characteristics from each event category are described in Section 5. The ranges for each type of event are described for RPAD and frequency events in Section 5.1 and Section 5.2, respectively.

2 Screening Algorithm Development

This section describes the algorithm developed to screen PMU data taken from PMUs within the UT-Austin Independent Texas Synchrophasor Network for power system events. The PMU synchrophasor data consist of voltage magnitude, phase angle, and frequency for each PMU station and are saved hourly in CSV format. All PMU frequencies and all possible voltage phase angle separations between PMU stations are analyzed. A flowchart describing the algorithm is shown in Figure 4. In the flowchart, the signal to be analyzed for the hourly PMU file uploaded is assigned to the variable *y*. The algorithm does not analyze the entire hour of data at once, but instead analyzes a window of PMU data, assigned to the variable *yWindow*. The subroutine analysis on the window of data *yWindow* is applied for each moving window of data until the end of the entire hour of the signal *y* is reached.

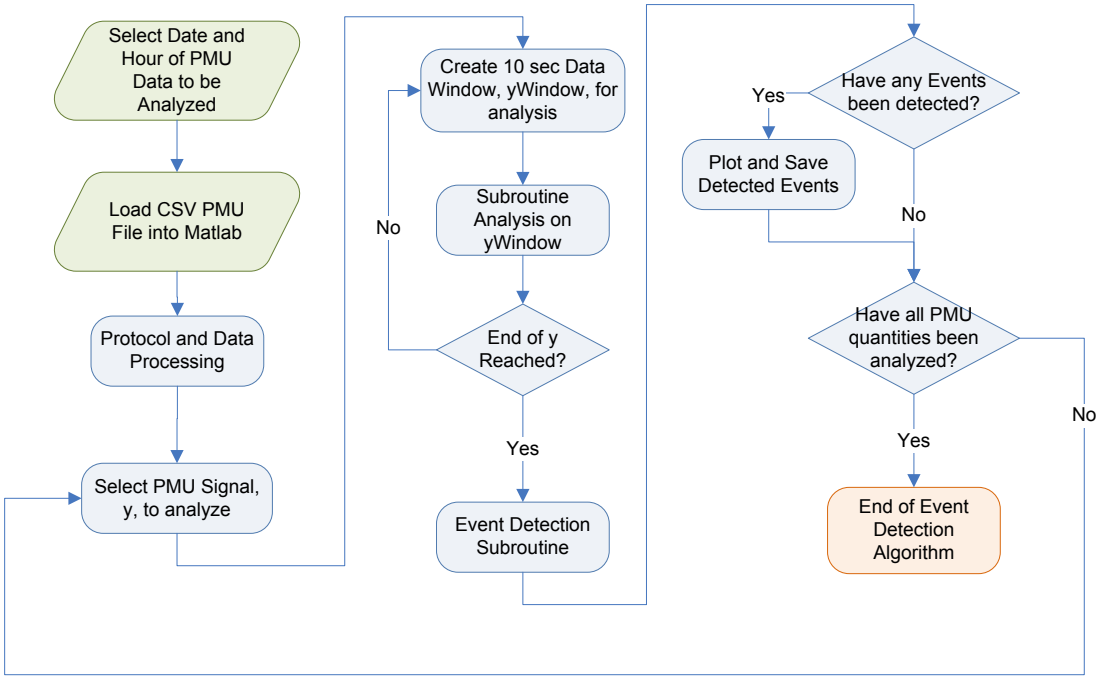

Figure 4. Flowchart of the processes used to screen for events in PMU data

In Section 2.1, the PMU CSV format and the protocol created to organize and label PMU data for analysis is described. Section 2.2 describes the methods used to screen for events in the data. Four different methods were used because each method is able to detect different types of events. The methods are fast Fourier transform (FFT); matrix-pencil, an analysis based on the difference between the minimum value and maximum value within a window of data (min-max method); and Yule-Walker. FFT and Yule-Walker are spectral methods, whereas matrix-pencil is parametric. All methods are applied to a window of PMU data where resulting peak values from each method applied to the data window are saved. The peak values from each data window for the entire PMU file are used to detect events. Any peak magnitudes greater than three standard deviations are marked as possible events. Section 2.3 describes how the results from each of the methods are used to detect events. If two or more methods detect an event in the same

data window, that window is marked as containing an event. The event is plotted and data saved for further analysis. The algorithm was developed in Matlab and uses functions from the Signal Processing Toolbox and user-defined functions [5].

2.1 PMU Data Format and Protocol

New PMU stations are installed and removed from the network for various reasons, causing the format of the archived hourly PMU files to constantly change. The grouping of PMU quantities for each station changes as well, resulting in two types of data files. The two types of data files are shown in Table 1 and Table 2. The voltage magnitudes were arbitrarily selected. All measurements are taken at customer-level voltage of 120 V.

Table 1. An example of Type 1 PMU Data in CSV Format for Two PMU Stations With the Magnitude, Angle, and Frequency for Each Station Grouped Together

t	MAG1 (V)	ANG1 (deg)	FREQ1 (Hz)	MAG2 (V)	ANG2 (deg)	FREQ2 (Hz)
…	…	…	…	…	…	…
24:26.7	79924.90	120.18	59.98	40.80	-10.12	60.02
24:26.8	79930.60	119.89	59.98	40.81	-9.91	60.02
24:26.8	79933.17	119.60	59.98	40.82	-9.70	60.02

Table 2. An Example of Type 2 PMU Data in CSV Format for Three PMU Stations With the Frequencies for Each Station Listed in the Last Columns

t	MAG1 (V)	ANG1 (deg)	MAG2 (V)	ANG2 (deg)	MAG3 (V)	ANG3 (deg)	FREQ1 (Hz)	FREQ2 (Hz)	FREQ3 (Hz)
…	…	…	…	…	…	…	…	…	…
08:38.6	41.192	-22.827	79166.508	-45.7	73482	99.924	59.949	59.947	60.008
08:38.7	41.192	-23.457	79141.992	-46.3	0	0	59.948	59.947	0
08:38.7	41.187	-24.068	79138.844	-46.9	73484.742	100.14	59.948	59.948	60.009

Because of the two file types and the large variety in the number and location of stations in operation, it is cumbersome to read PMU data and begin analysis of the data. Without an automated method, it is first necessary to open the PMU file and count the number of stations and the order of the stations to conduct an accurate analysis. In addition, dropped data points appear in the voltage magnitude and frequency as zeros and need to be removed before analysis can begin.

A protocol was created to analyze the PMU data files and indicate the type of file format, the number of PMU stations, and the quality of the PMU data. The file format type indicates if the PMU frequency for each station is grouped with the other PMU station data or if all PMU frequencies are grouped together, as shown in Table 1 and Table 2, respectively. The number of PMU stations provides the number of PMU stations in operation at the time the data was archived. The quality of the PMU data is "true" if the

PMU station contains zero or a limited number of dropped data points and "false" if the data contains many dropped data points or if the PMU station is not sending data to the phasor data concentrator. The Protocol function determines the PMU file type and the number of PMU stations. It also indicates the column locations for each PMU station's magnitude, angle, and frequency data, and if the PMU data is "false" or contains missing data. An example is shown in Table 3. This information is used to determine how to label the data type and how to label the data by PMU location.

Table 3. An Example of the Protocol Function Output

Type	Number of Measurement Points (NMP)	NMP 1					
		Mag		Ang		Freq	
		Col Index	Fault	Col Index	Fault	Col Index	Fault
2	6	1	"true"	2	"true"	13	"true"

After the file format type is known, the columns of the PMU data are identified and the voltage phase angle data is modified before analysis begins. Because the rotation of the voltage phasors is not constant and not at nominal frequency (60 Hz), the voltage phase angle increases or decreases depending on if the speed of rotation is greater or less than nominal. When the voltage phasor is rotating at greater-than-nominal speed and crosses from 180 to -180 degrees, the voltage phase angle jumps, as shown in Figure 5. The voltage phase angle at each PMU station is unwrapped before the difference in the voltage angle between the two stations is taken. The unwrapped RPAD is shown in Figure 6 and can now be screened for events. All possible RPAD combinations are considered for each PMU file.

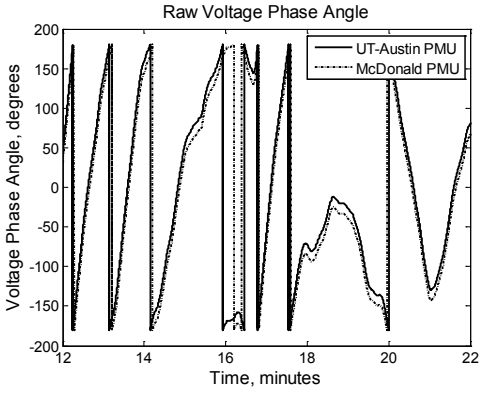

Figure 5. Raw voltage phase angle for two PMU stations

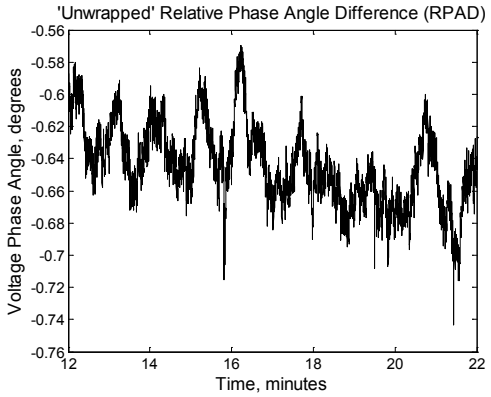

Figure 6. RPAD between the same two PMU stations corrected by individually unwrapping and taking the difference

To illustrate the amount of information present in PMU data, an entire day of PMU RPAD data between UT-Austin and McDonald is plotted in Figure 7. Each PMU RPAD and frequency data set is screened for possible events. Section 2.2 describes the methods used to screen for events in the PMU data.

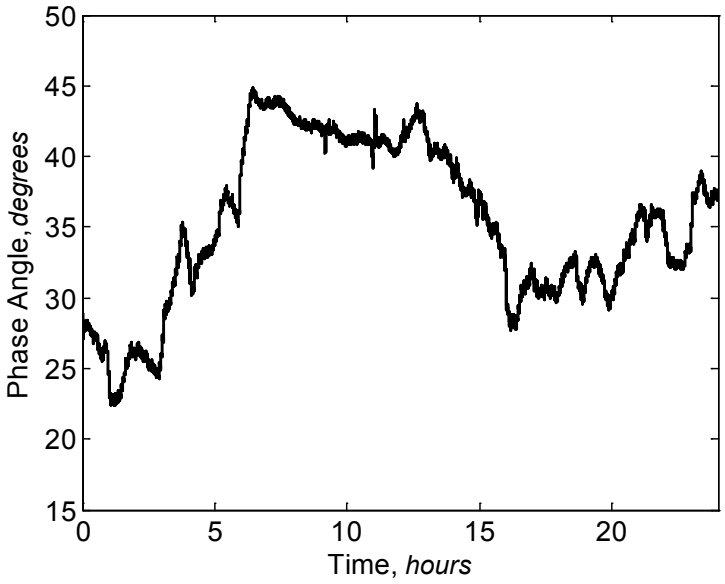

Figure 7. Voltage RPAD between UT-Austin and UTPA for 24 hours

2.2 Event-Screening Methods

To screen for events within each hourly PMU file, an overlapping, moving window is applied to the PMU data. The window size is 10 seconds long and overlaps half of the previously windowed data. The moving window method is illustrated in Figure 8.

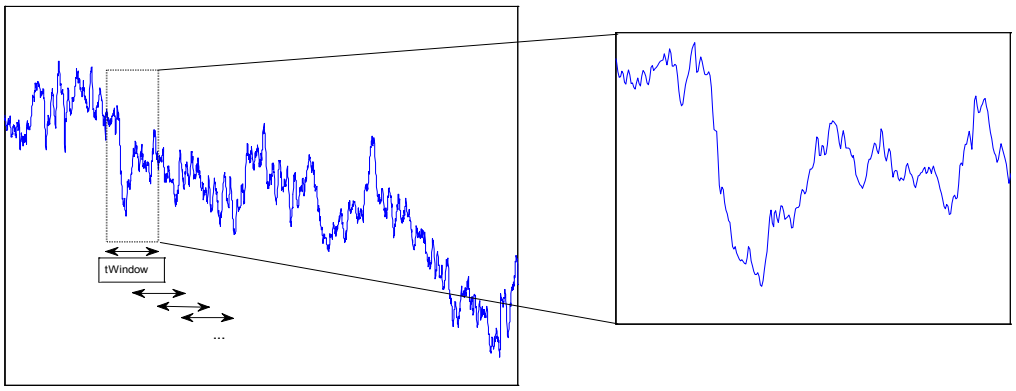

Figure 8. (Left) An illustration of a moving window applied PMU data and (right) a 10-second data window for analysis

Each window of data is analyzed for possible events by applying the four different detection methods mentioned. All methods except for the min-max are based on the strength of the estimated frequency content. Only frequencies below 2 Hz are examined (the frequency range of inter- and intra-area oscillations [6]). Each method is described in detail below.

2.2.1 FFT

Before the method is applied, the data window is differentiated using the Matlab function `diff` to remove dc offset in the data to facilitate the detection of events in the low-frequency range below 1 Hz. Differentiating the data increases the noise in the data; however, it has been found that the magnitude of frequencies associated with events in the data tend to be very high. Therefore, increased noise is not a concern for this analysis.

The FFT utilizes the Matlab function `fft` to detect events in the PMU data. This function returns the discrete Fourier transform calculated using the FFT algorithm. The discrete Fourier transform is used to find the strongest frequency component within the data window. The maximum amplitude, $|Y(f)|$, is saved for frequencies in the range of $0 < f \leq 2\ Hz$. The method is applied to a data window of the voltage phase angle in Figure 9 containing oscillations induced by a large event. The discrete Fourier transform applied to the data window containing event information is shown in Figure 10. The Fourier transform in Figure 10 shows a strong 0.64-Hz component. In the algorithm, the peak magnitude, $|Y(f)| = 0.03$, would be saved for this data window.

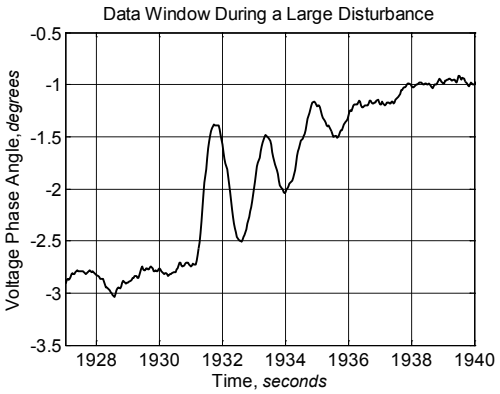

Figure 9. Window of voltage RPAD

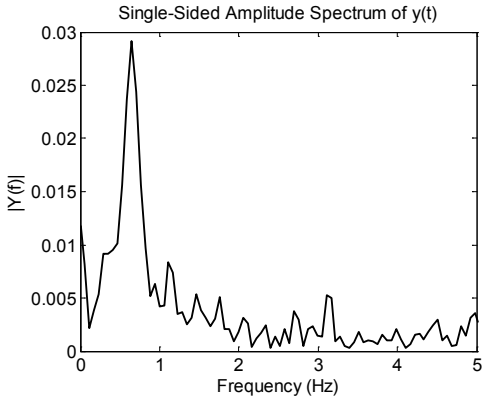

Figure 10. Amplitude of spectrum of voltage RPAD

The FFT method is applied to each 10-second data window for the entire hour of PMU data. The average and standard deviation are calculated for all saved peak magnitudes. Any saved magnitudes above three standard deviations are tagged as possible events. Three standard deviations window was selected based on examples of detected events from the UT synchrophasor network data. A plot of the peak magnitudes from each 10-second data window is shown for an hour of PMU frequency in Figure 11. The average and standard deviation of the peak magnitudes are indicated. The outliers, or possible events, are also marked in Figure 11.

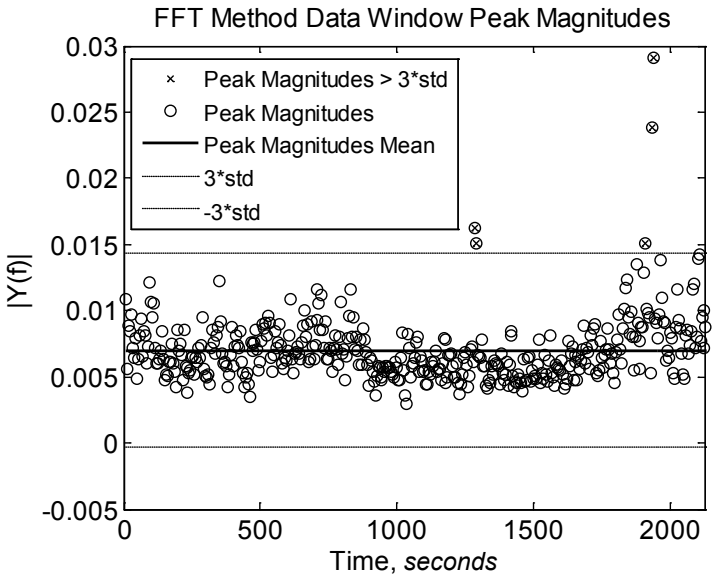

Figure 11. In the FFT method, data windows during which the peak magnitude exceeds three times the standard deviation of peak magnitudes for the entire hour are marked with an x.

2.2.2 Matrix-Pencil

The matrix-pencil method [7] fits a sum of damped sinusoids to evenly sampled PMU data. The amplitude, phase angle, frequency, and damping are the parameters of the damped sinusoids estimated to fit the PMU data. The mathematical representation of the sum of damped sinusoid estimates fitted to the sampled data is given in (1).

$$y(k) = \sum_{i=1}^{n} R_i z_i^k \qquad \textbf{(1)}$$

where the discrete signal $y(k)$ in (3) is equal to the sum of the product of the residues or complex amplitudes R and the poles z. The parameter n is the number of sinusoids or modes to be estimated. The damping and frequency estimates of the signal can be extracted from each z_i, as shown in (2).

$$\begin{aligned} z_i &= \exp(\lambda_i \Delta t) \\ \lambda_i &= \sigma_i \pm j\omega_i \end{aligned} \qquad \textbf{(2)}$$

This method also utilizes singular value decomposition to remove noise from the signal before the estimates are made. Because a matrix-pencil function is not available in Matlab, a user-defined function was created to calculate the parameters using the matrix-pencil method and is described briefly by the following equations.

A matrix [Y] is created from the noisy PMU data $y(k)$, as shown in (3).

$$[Y]=\begin{bmatrix} y(0) & y(1) & \dots & y(L) \\ y(1) & y(2) & \dots & y(L+1) \\ \dots & \dots & \dots & \dots \\ y(N-L-1) & y(N-L) & \dots & y(N-1) \end{bmatrix} \quad \textbf{(3)}$$

The parameter *L* is the pencil parameter, and *N* is the total number of data points in $y(k)$. Singular value decomposition is applied to [Y], as shown in (4).

$$[Y]=U\Sigma V^{H} \quad \textbf{(4)}$$

The matrices *U* and *V* are unitary matrices, and the operator *H* is the conjugate transpose. The singular values of [Y] are located along the diagonal of matrix Σ in descending order. A threshold value is selected so that the *n* singular values above the threshold are considered and used to create the following matrices.

$$\begin{aligned} [V'] &= [v_1, v_2, \dots, v_n] \\ [Y_1] &= U\Sigma'[V_1']^{H} \\ [Y_2] &= U\Sigma'[V_2']^{H} \end{aligned} \quad \textbf{(5)}$$

The *v*s are the column vectors of *V* from (4), matrix Σ' is the first *n* columns of Σ, $[V_1']$ is the matrix *V* with the final column removed, and $[V_2']$ is the matrix *V* with the final row removed. Using the matrix-pencil as defined in [7], the matrices from (5) can be used to create the following new matrix-pencil definition for noisy data.

$$[Y_1]^{+}[Y_1] = V_2'^{H}\left[V_1'^{H}\right]^{+} \quad \textbf{(6)}$$

The next step is to find the eigenvalues for $V_2'^{H}\left[V_1'^{H}\right]^{+}$. The eigenvalues are used to solve for *R* from (1) and is rewritten in the following format.

$$\begin{bmatrix} y(0) \\ y(1) \\ \vdots \\ y(N-1) \end{bmatrix} = \begin{bmatrix} 1 & 1 & \dots & 1 \\ z_1 & z_2 & \dots & z_n \\ \dots & \dots & \dots & \dots \\ z_1^{N-1} & z_2^{N-1} & \dots & z_n^{N-1} \end{bmatrix} \begin{bmatrix} R_1 \\ R_2 \\ \vdots \\ R_n \end{bmatrix} \quad \textbf{(7)}$$

The estimates for the damping and frequency are extracted from *z*, as shown in (2), and the amplitude is extracted from *R*.

The matrix-pencil method is applied to a 10-second window of PMU data. Figure 12 shows the reconstructed signal (solid line) using the estimated parameters compared to the original signal (dotted line). Because noise was removed using singular value decomposition, parameters were not estimated to fit the noise but only the "true" modes present in the data.

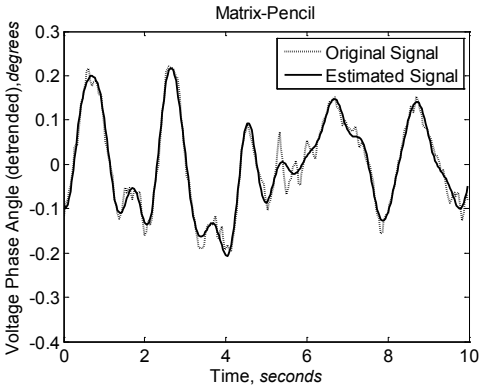

Figure 12. An example of the matrix-pencil method used to estimate parameters of the de-noised signal

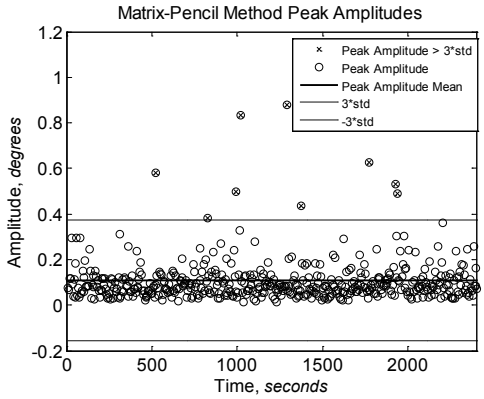

Figure 13. In the matrix-pencil method, data windows during which the peak magnitude exceeds three times the standard deviation of peak magnitudes for the entire hour are tagged.

The values of the two highest estimated amplitudes are saved for each data window. The method is repeated for the entire hour of data. It is assumed that if an event is present in the data, the max amplitude would be significantly larger than the max amplitude from a data window without any events. After the two highest magnitudes are saved for all data windows, the averages and standard deviations for the highest and second highest magnitudes are calculated separately. Detection of possible events is similar to the FFT method; any magnitudes above three standard deviations are tagged as possible events, as shown in Figure 13.

2.2.3 Yule-Walker Spectral

The Yule-Walker spectral method is similar to the FFT method but utilizes the `pyulear` function from the Matlab Signal Processing Toolbox [5]. The `pyuler` function calculates the power spectral density (PSD) using the autoregressive Yule-Walker method. The PSD for a data window containing an event is shown in Figure 14.

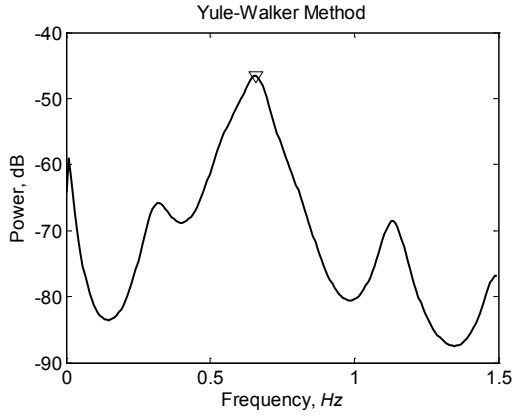

Figure 14. Yule-Walker method power of frequency content in PMU signal during a large disturbance

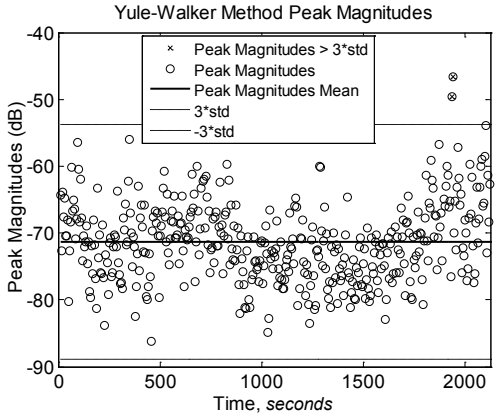

Figure 15. In the Yule-Walker method, data windows during which the peak magnitude exceeds three times the standard deviation are tagged.

The peak value in the PSD in dB is marked. The peak values for each PSD of the data window are saved. This is repeated for the entire hour. The average and standard deviation of the maximum magnitudes are calculated. Magnitudes above three standard deviations are tagged as possible events, as shown in Figure 15.

2.2.4 Min-Max

For this method, the difference between maximum and minimum values within the data window is calculated. The difference for each data window for the entire hour is saved. This method is sensitive because it also detects gradual changes in the signal above the 10-second data window that are not caused by power system events. Possible events are detected by calculating the average and standard deviation for all the data window differences for the entire hour of PMU data. The differences that exceed three times the standard deviation are marked as possible events, as shown in Figure 16.

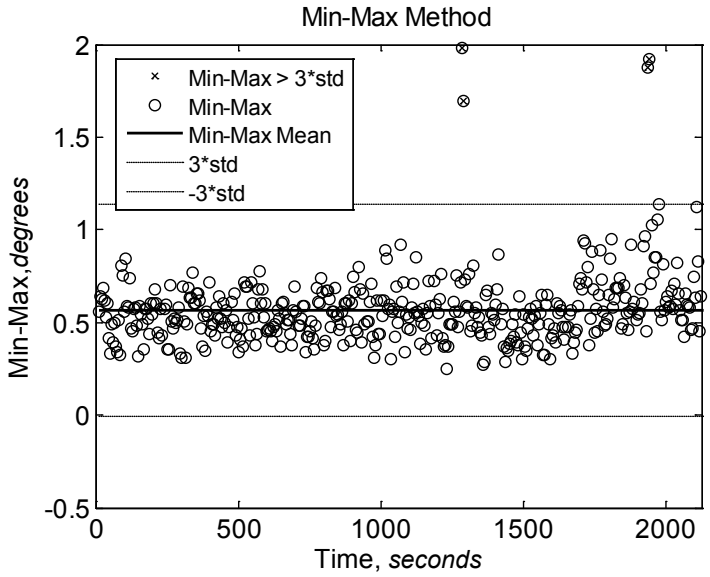

Figure 16. In the min-max method, data windows during which the difference between the minimum and maximum values in a 10-second data window exceeds three times the standard deviation are tagged.

2.3 Method Results for Marking Events

After all methods have been used to screen for possible events in the PMU data, the time stamps of data windows marked as containing possible events are compared. Figure 17 shows an example of the results for possible events in the RPAD between UT-Austin and McDonald. If two or more methods detect a possible event in the same data window, that data window is marked as containing an event and the PMU data for that window is saved and plotted. In Figure 17, an event is detected at 1,285 seconds by both the matrix-pencil and min-max methods. Another event is detected at 1,935 seconds by all four methods. This event is analyzed further in Section 3.1.

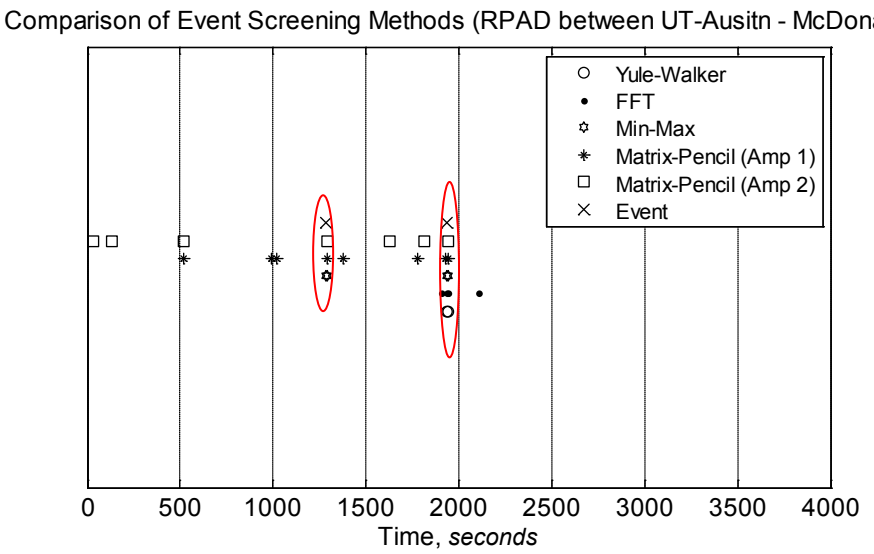

Figure 17. Comparison of all the screening algorithms

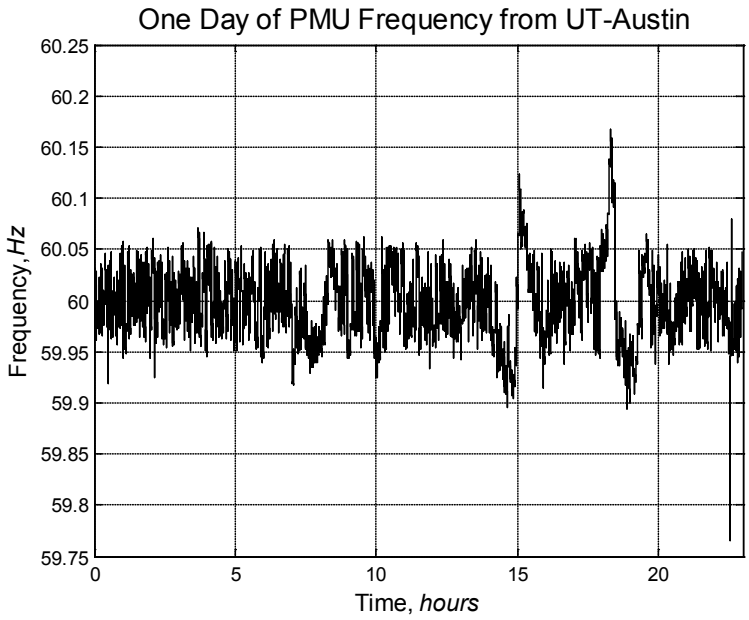

Figure 18. An entire day of PMU frequency from UT-Austin

3 Application and Demonstration

The results from the algorithm are examined by screening 24 hours (00:00 to 23:59 UTC) of PMU data for power system events. The UT-Austin PMU and McDonald PMU were operational during this time period. *The voltage RPAD between UT-Austin and McDonald and the frequencies at each location are analyzed*. An example of 24 hours of UT-Austin PMU frequency is shown in Figure 18 to illustrate the difficulty of visually screening for events in PMU data. The PMU frequency is a calculated quantity that is based on the measured voltage phase angle [8] and differs slightly across the power system, as shown in the PMU frequencies in this section. High-precision PMU calculated frequencies also provide more information than a single-system frequency.

Two types of events found in the data are described here to illustrate how the screening algorithm detects events. The first event (described in Section 3.1) was caused by a sudden loss of generation. The event occurred at 23:33 UTC (17:33 CST) and is visible in all three signals. The second event (described in Section 3.2) was probably caused by a recloser operation visible only in the McDonald PMU data. Strong oscillations visible only at the UT-Austin PMU are also examined in Section 3.2. The source of the oscillations in the UT-Austin PMU data is unknown.

3.1 Screening Results for a Systemwide Event Caused by Loss of Generation

At 23:33 UTC, a generating unit tripped, resulting in a loss of 810 MW of generation and a frequency decline to 59.774 Hz. The ERCOT load at the time was 35,000 MW [3]. The frequency at UT-Austin and McDonald are screened for events using the methods described in Section 2. The results from the algorithm are shown in Figure 19 and Figure 20. The generating unit trip was the only event detected in both PMU frequencies and was detected by all four methods in the UT-Austin PMU frequency, as shown in Figure 19. As shown in Figure 20, the disturbance was detected and tagged in the McDonald PMU frequency, but the matrix-pencil method detected other possible events as well (represented in Figure 20 as □ and ✶). However, because the matrix-pencil method was the only method to detect a possible event, these data windows were not tagged as real events.

The PMU frequencies data window for the event is plotted in Figure 21. Both PMU frequencies decline to 59.76 Hz, which differs slightly from the ERCOT Grid Report [3] frequency decline possibly because the PMU frequencies are taken at specific buses rather than representative of the system frequency. It is possible that the PMU data also has a higher resolution than the ERCOT data.

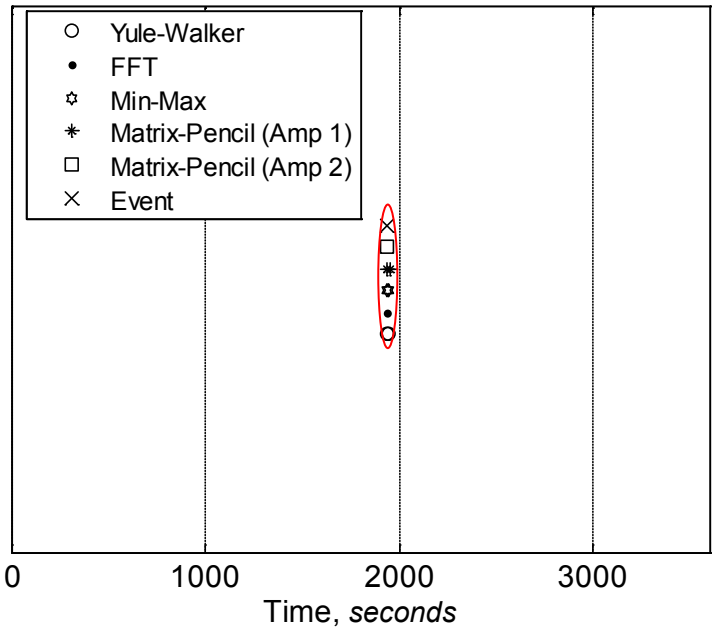

Figure 19. Events detected in the UT-Austin PMU *frequency* for 23:00 UTC

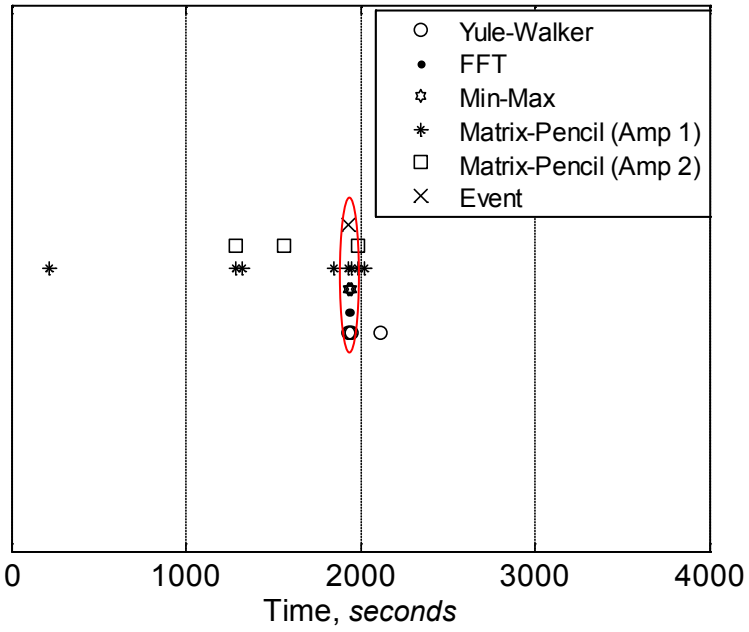

Figure 20. Events detected in the McDonald PMU *frequency* for 23:00 UTC

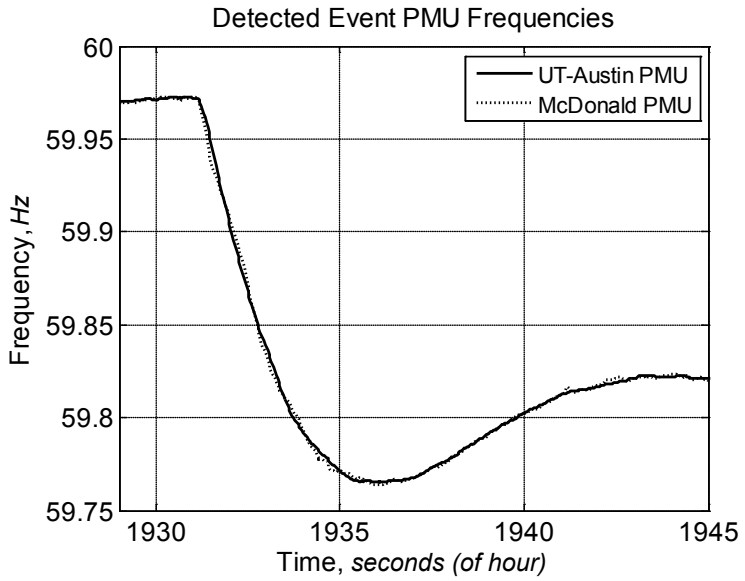

Figure 21. A large disturbance caused by a sudden 810-MW loss-of-generation impact on the UT-Austin PMU and McDonald PMU frequencies

The same generating unit trip was detected in the RPAD between UT-Austin and McDonald, as shown in Figure 22. An additional event was detected in the RPAD signal, but it is not clear if it is an actual event or if the threshold values in the algorithm are too sensitive. The RPAD during the event is plotted in Figure 23. The voltage phase angle has an approximate initial upswing of 1.5 degrees. The amplitude of the oscillation is not very large, and it is possible that the location of the generating unit that tripped is located far from the UT-Austin and McDonald PMU stations. The oscillations in the voltage phase angle prior to and after the event are much smaller and have an amplitude between 0.1 to 0.25 degrees.

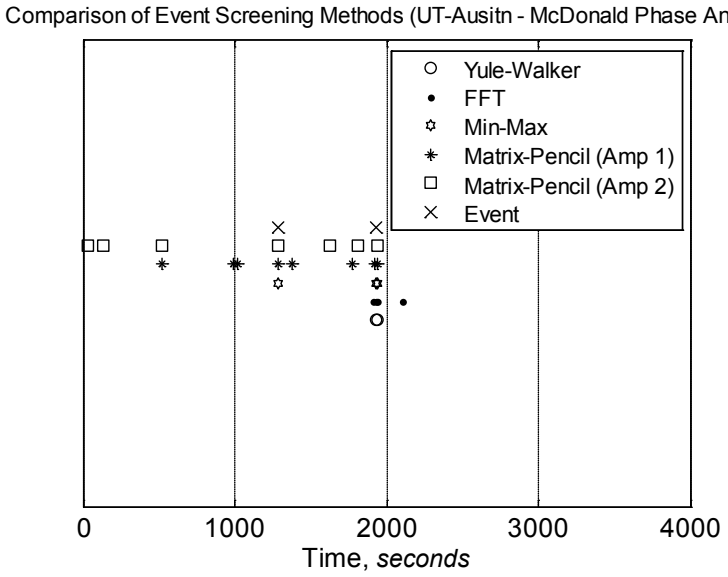

Figure 22. Events detected in the *voltage RPAD* between UT-Austin and McDonald PMU for 23:00 UTC

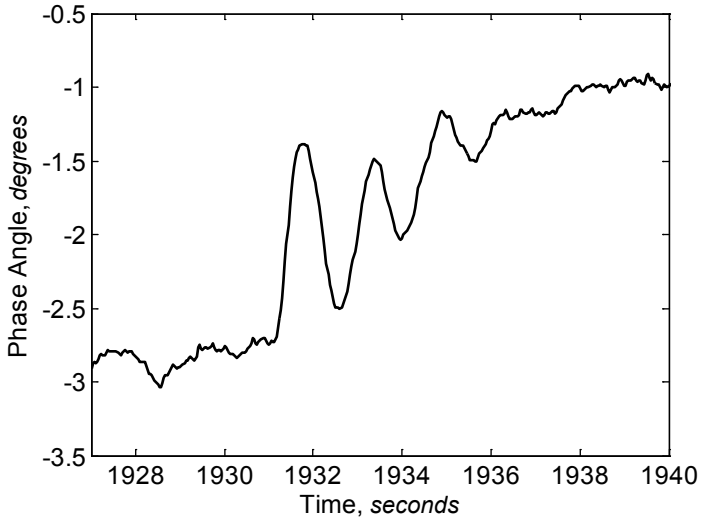

Figure 23. A large disturbance caused by a sudden 810-MW loss-of-generation impact on the *voltage RPAD* between UT-Austin and McDonald

The examples illustrate that the screening algorithm can very easily detect a large event in all the PMU signals analyzed. Screening for smaller events in the PMU data are examined next.

3.2 Screening Results for Local Events With Unknown Causes

The methods are further evaluated by screening PMU frequencies and RPAD data for smaller, local events. In this section, an hour of PMU data (17:00 UTC) is screened for possible events. The algorithm is applied to the UT-Austin PMU frequency, and the McDonald PMU frequency with results is shown in Figure 24 and Figure 25.

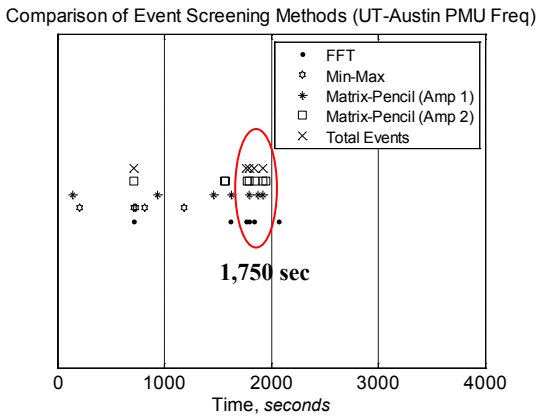

Figure 24. Events detected in the UT-Austin PMU frequency for 17:00 UTC

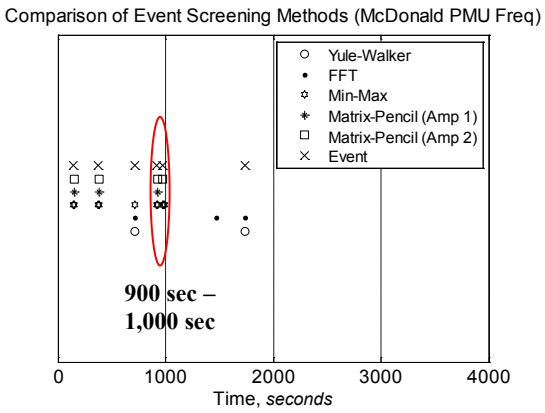

Figure 25. Events detected in the McDonald PMU frequency for 17:00 UTC

Many of the events detected in the UT-Austin PMU frequency were not detected in the McDonald PMU frequency and vice versa. In the UT-Austin PMU frequency, the events detected starting at approximately 1,750 seconds are strong oscillations that are not visible in the McDonald PMU frequency. For comparison, a 20-second window of frequency data is plotted in Figure 26. The UT-Austin frequency (solid line) has stronger, higher-magnitude oscillations, but it is difficult to identify the strength and frequency of the oscillations based on the plot.

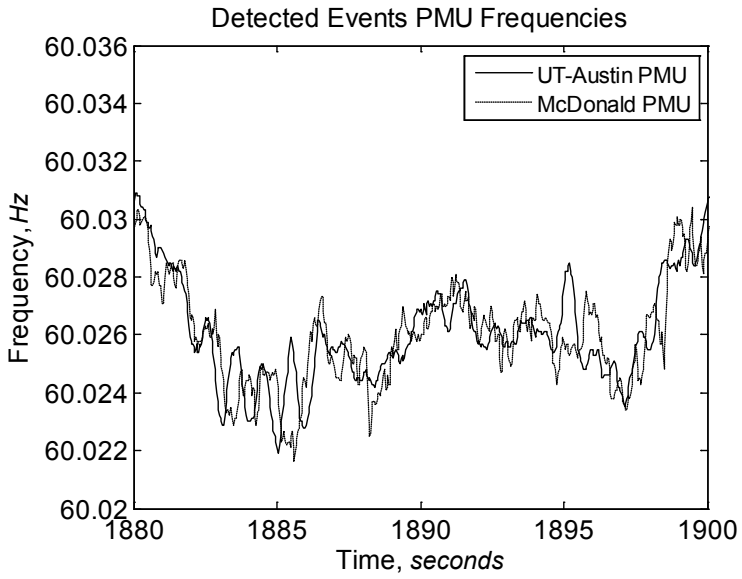

Figure 26. A small-disturbance event detected in the UT-Austin PMU frequency but not in the McDonald PMU frequency

The PSD is calculated to analyze the strength and frequency of the oscillations present in the PMU data. The PSD is stored for each 10-second window and plotted as a contour plot to compare the frequency content of the UT-Austin and McDonald PMU signals. The contour plots are shown in Figure 27. From Figure 27, it is easy to see a strong, 1-Hz

oscillation in the UT-Austin PMU frequency that is not visible in the McDonald PMU frequency for the same time period. The oscillation in the UT-Austin data is strongest from approximately 1,600 seconds to 2,000 seconds, as indicated by the dark red. This is approximately the same time period that the algorithm tagged as a possible event. A 1-Hz oscillation indicates intra-area oscillations [6] (usually associated with a single machine), but the exact cause of the 1-Hz oscillation is currently unknown. In the contour plot, the frequency on the y-axis is the frequency content of the PMU frequency signal. The PMU frequency is not measured, but calculated from the voltage angle.

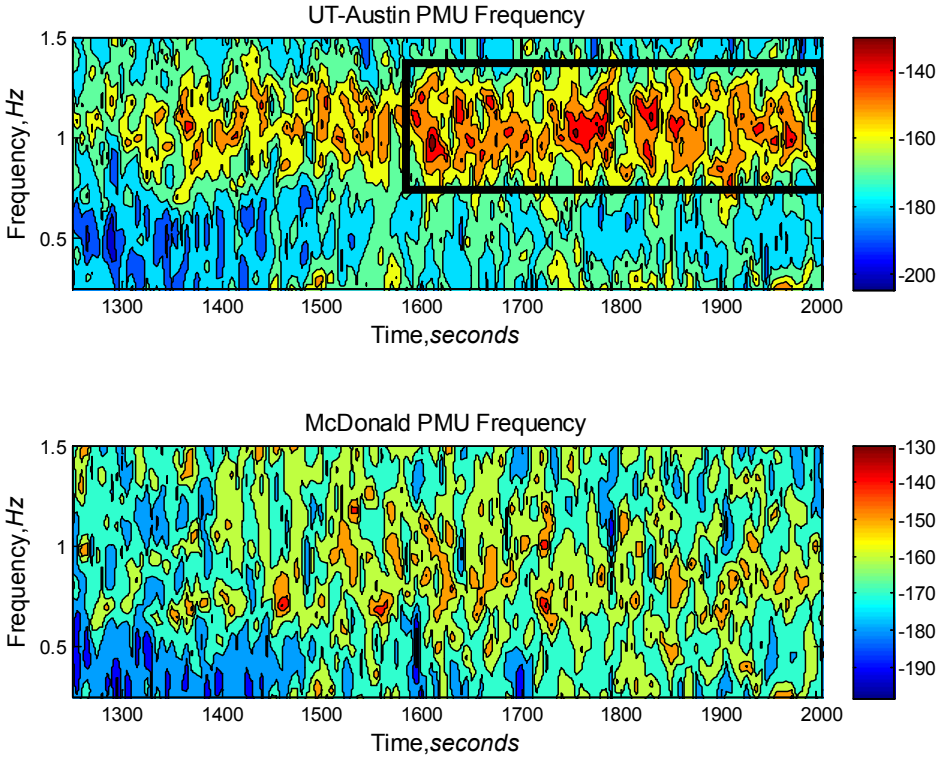

Figure 27. A contour plot of the PSD (low-frequency content over time) shows (top) a 1-Hz oscillation present in the UT-Austin PMU frequency signal, but (bottom) the 1-Hz oscillation is absent in the McDonald PMU frequency signal.

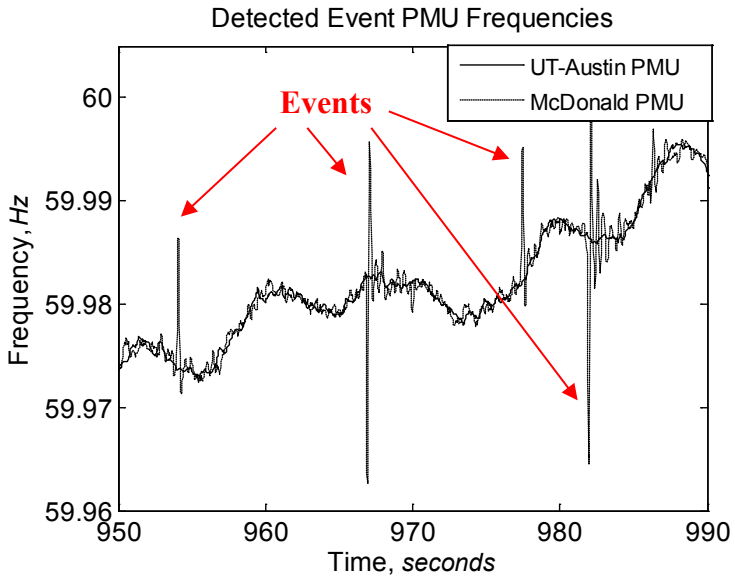

Figure 28. (Dotted line) A small-disturbance event detected in the McDonald PMU frequency but (solid line) not in the UT-Austin PMU frequency

In the McDonald PMU frequency, the events detected starting at approximately 900 seconds are damped oscillations that are not visible in the UT-Austin PMU frequency. A 40-second window of frequency data is plotted in Figure 28. The (dotted line) McDonald PMU frequency contains many damped oscillations that are not present in the (solid line) UT-Austin PMU frequency. The cause of these oscillations will become apparent when examining the voltage phase angle.

The screening results for PMU RPAD data for one hour (17:00 UTC) is shown in Figure 29. The algorithm is able to detect events that were seen in the McDonald PMU frequency at approximately 900 seconds to 1,000 seconds, shown in Figure 25 and Figure 28. However, the events detected in the UT-Austin frequency at approximately 1,750 seconds to 2,000 seconds (refer to Figure 24) were not as clearly visible in the voltage phase angle. The FFT and matrix-pencil methods were able to detect the oscillation during the 1,750-second to 2,000-second time frame, but because these methods did not detect the oscillation simultaneously, they were not tagged as events in the results from the PMU RPAD analysis.

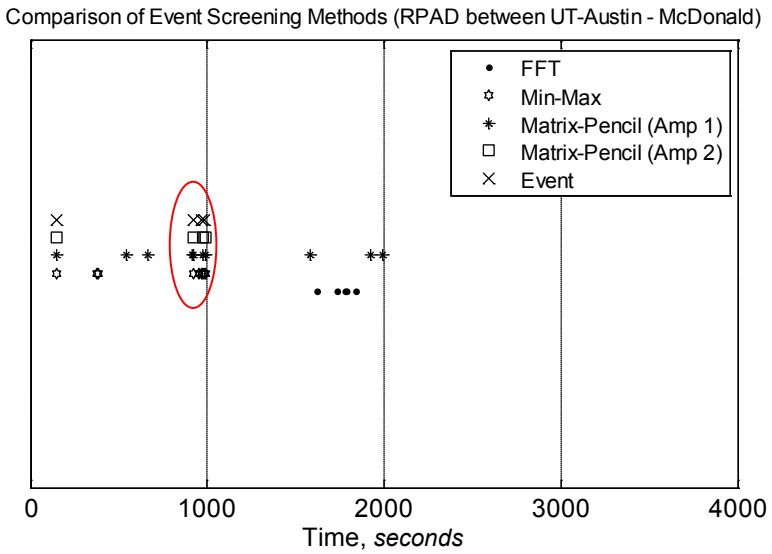

Figure 29. Events detected in the UT-Austin to McDonald PMU voltage phase angle difference for 17:00 UTC

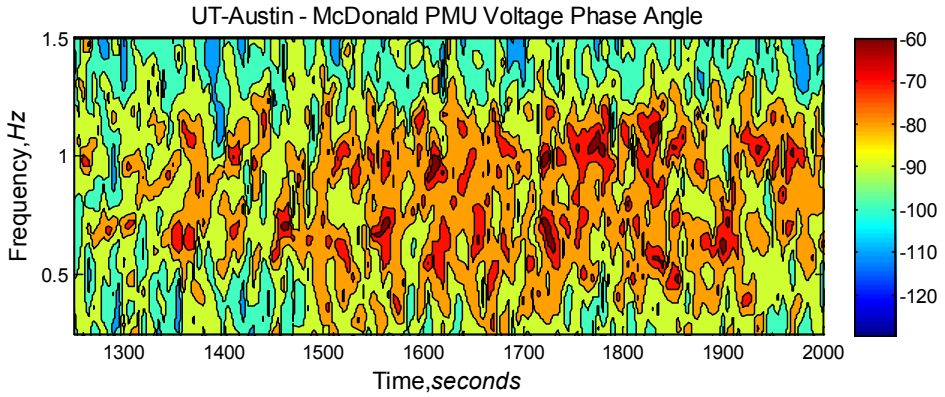

Figure 30. A contour plot of the PSD (low-frequency content over time) in the voltage RPAD over time shows a strong 1-Hz oscillation as well as another 0.6-Hz to 0.7-Hz oscillation.

The contour plot for the RPAD signal in Figure 30 indicates that the 1-Hz oscillation is strong during the same time period, as shown in (top) Figure 27, but contains an approximate 0.6-Hz to 0.7-Hz oscillation as well. The contour plot for the entire hour of data shows that the 1-Hz oscillation is not as strong at other times.

The events detected in the McDonald PMU frequency in Figure 28 were also detected in the PMU voltage phase angle. The RPAD between UT-Austin and McDonald for this series of events is plotted in Figure 31. The sudden change and return of the phase angle indicates multiple reclosing events. Because the oscillations are visible only in the McDonald PMU frequency, it is assumed that the event occurred near McDonald (local event). However, it is difficult to tell at what voltage level the recloser is located (distribution or transmission voltage level). It can be concluded that the recloser is most likely not located at a distribution feeder directly upstream from the PMU station,

otherwise a reclosing event could cause the PMU to lose power and the PMU would be unable to measure and transmit voltage phasor data. The measured voltage magnitude at McDonald is too noisy to extract any conclusions.

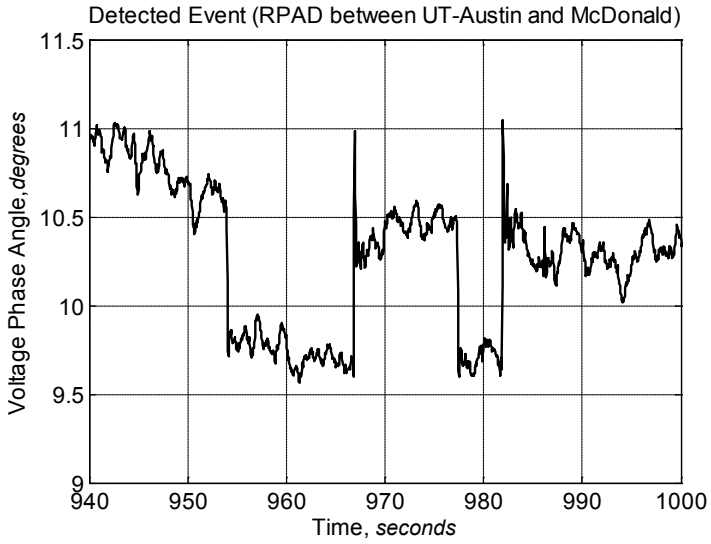

Figure 31. A small-disturbance event detected in RPAD between the UT-Austin and McDonald PMUs

So far in this report, the algorithm used to screen PMU data generated by the UT-Austin synchrophasor network for power system events has been described. The algorithm uses four different methods to screen for possible events. Each method is applied to a moving window of PMU data. Any values from each method that exceed three standard deviations away from the mean are marked as possible events. A data window is marked as containing an event if two or more methods detect a possible event in the same data window. In the following sections, events detected using this method are examined further. The event-screening algorithm is applied to many days' worth of PMU data, and all detected events are collected. Events are placed into categories based on common characteristics. These categories and common characteristics are examined further in Section 4 and Section 5.

4 Event Categorization Based on Visual Analysis

This section discusses the categorization of events detected by the screening algorithm based on common visual characteristics. The event categorizes and examples from each are described and provided in Section 4.1. In Section 4.1.1 and Section 4.1.2, the events as seen in the RPAD and frequency data are described, respectively. Example events from the PMU data are provided as well.

4.1 Event Categories

The categories of detected events for RPAD and frequency signals are proposed in Table 4 below. Events were extracted from nine days' worth of data taken from different seasons of the year and from different years (from 2010 to 2012). Based on the types of events extracted from these days, the categories were selected using common visual characteristics (oscillations, impulses, step change, and rate of change). The RPAD has three categories with a total of seven subcategories. The frequency also has three categories with a total of seven subcategories.

Table 4. Categories Presented for PMU RPAD and Frequency Events

Voltage RPAD		Frequency	
Category	*Subcategory*	*Category*	*Subcategory*
Impulse	Single (Small)	Impulse	Small
	Single (Large)		Large
Transient	Damped	Transient	Damped
	Sustained		Sustained
Step Change	Momentary (Small)	Rise or Drop in Frequency	Rise
	Momentary (Large)		Drop
	Sustained		Unit Trip

Although the main categories were based on visual inspection, the subcategories were created after the quantitative characteristics from each category were extracted. The subcategories allow for more precise selection of thresholds when determining the category and subcategory of an event in the PMU data. The categories and subcategories are explained in more detail for the RPAD and frequency in Section 4.1.1 and Section 4.1.2, respectively. The typical ranges for each category are given in Section 5.1.1.1 and Section 5.2.1.1.

4.1.1 Voltage RPAD Event Categories

The event categories in the voltage RPAD are presented here, with examples shown for each category. The RPAD is approximately proportional to the real power flow between two buses. A sudden change in the RPAD indicates a sudden change in power flow somewhere between the two buses. The events presented here are those in which the RPAD behavior suddenly changes. When this occurs, it is assumed that the power flow

somewhere between the two PMU measurements changes as well. In the case of an impulse event, the power flow change typically occurs near only one of the PMU stations, as explained in Section 4.1.2. This may be interpreted as a sudden surge or drop of power caused by the energizing of a motor or transformer or other switching event where the power quickly returns to pre-event conditions. Step change events may be interpreted as a shift in power caused by events such as a transmission line trip or a generating unit trip. The cause of transient events at this time is unknown, but one possibility is that they may be caused by some switching event that occurs at a distance from the PMU station and causes power flows throughout the system to oscillate with a higher magnitude change in the RPAD than during normal operating conditions. These oscillations are mostly within the mechanical time constant range of synchronous generator power plants within the area. The categories for the RPAD are examined in further detail below.

4.1.1.1 Impulse

The first event category is for an impulse event as detected in the RPAD signal. The duration of the impulse is very short and the change in the value of the RPAD varies. The rate of change of the RPAD during the impulse event is typically very high. Two examples of the event are presented below. The first impulse event, shown in Figure 32, falls under the single (large) subcategory and has a duration of 0.33 seconds (20 cycles) and a magnitude of 1.7 degrees. The ramp-up and -down rates are 15.9 deg/sec and 8.5 deg/sec, respectively. The ramp rates are approximations, and because of the 30-Hz sampling rate of the PMU data, higher frequency oscillations above 15 Hz are not recorded.

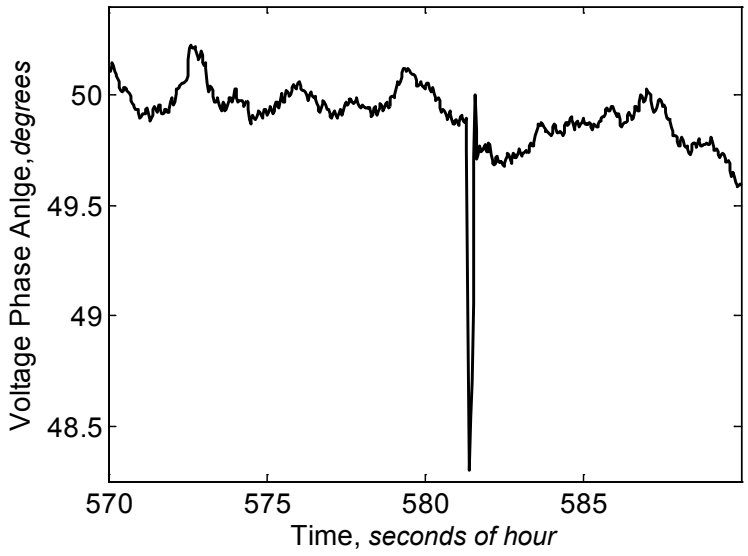

Figure 32. An example of an RPAD single (large) impulse event (RPAD between UT-Austin and McDonald)

This type of event occurs only at the McDonald PMU station, but the cause is unknown. After recording the time stamps of the occurrence of seven days' worth of impulse events, it was found that the event is not periodic. Impulse events seem to occur

randomly throughout the day. The impulse in the RPAD is thought to arise from a temporary imbalance in load and generation locally or might be caused by self-clearing faults. Analysis of probable causes of impulse events is described in Section 4.1.2 and Section 4.1.2.1.

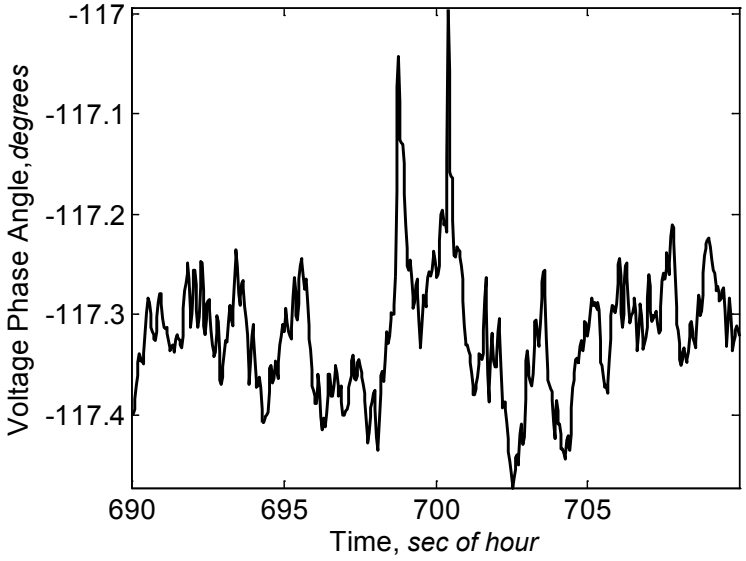

Figure 33. An example of an RPAD single (small) impulse event (voltage RPAD between UT-Austin and UTPA)

The second type of impulse event falls under the single (small) subcategory and is usually located near a peak of oscillations in the RPAD and sometimes appears as a pair of impulse events. This may also indicate a switching or reclosing event. Referring to Figure 33, the duration of the impulse event is 0.47 seconds (about 28 cycles) for the first impulse, occurring at 698.8 seconds; and 0.13 seconds (about 8 cycles) for the second impulse, occurring at 700.4 seconds. The change in angle is 0.25 degrees for the first impulse and 0.22 degrees for the second. The ramp-up and -down rates for the first impulse are 1.86 deg/sec and 0.64 deg/sec, respectively. The ramp-up and -down rates for the second impulse are 3.35 deg/sec and 2.44 deg/sec, respectively.

The impulse events shown in Figure 32 and Figure 33 are not caused by dropped data. Dropped data are detected by the screening algorithm but are also easy to identify visually because of the smoothness of the data (the RPAD would remain constant for the duration of the dropped data). The dropped data points are recorded as zeroes in the frequency data, which can also be used as a way to check if the detected event is actually an error in the data. Successful fault clearing may produce the phenomena indicated in Figure 33: two sequential events occurring two seconds apart.

4.1.1.2 Transient

The next event category is damped and sustained transients in voltage RPAD data. The causes of these events are unknown, but the common characteristic is higher magnitude oscillations compared to normal operating conditions. This low-frequency oscillation may indicate an oscillation between a large generator or group of generators near the

PMU station and the rest of system. These types of events differ from typical damped oscillations known as ambient response of the system that is typically seen in PMU data. The amplitude is typically larger and the oscillations during a transient event are not as noisy as ambient data. The duration, amplitude, and smoothness of the detected damped oscillation events vary as well. Three examples of damped transients are given below. The first damped transient event in Figure 34 lasts 5.07 seconds, and the amplitude of the largest swing is 0.41 degrees. The frequency of the oscillation is 1.17 Hz.

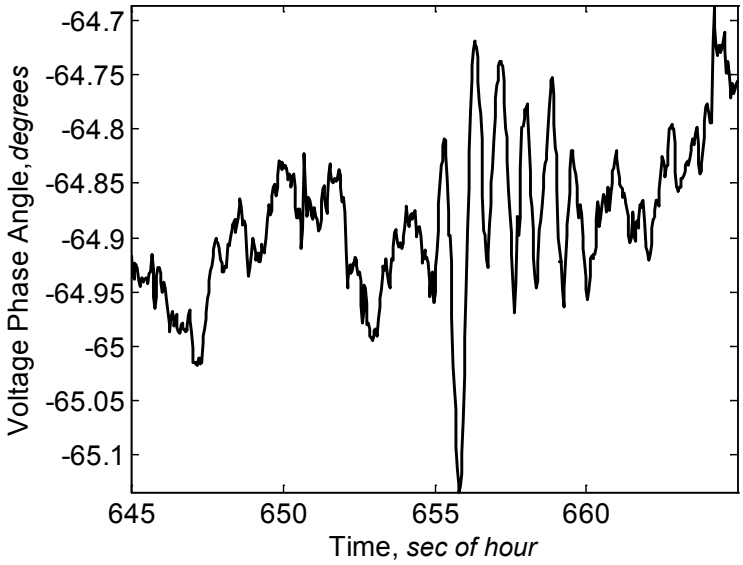

Figure 34. An example of an RPAD damped transient Event 1 (RPAD between UT-Austin and Waco)

In the damped transient event shown in Figure 35, the duration is 10.5 seconds and the largest swing is 1.01 degrees. The frequency of the oscillation is 0.59 Hz.

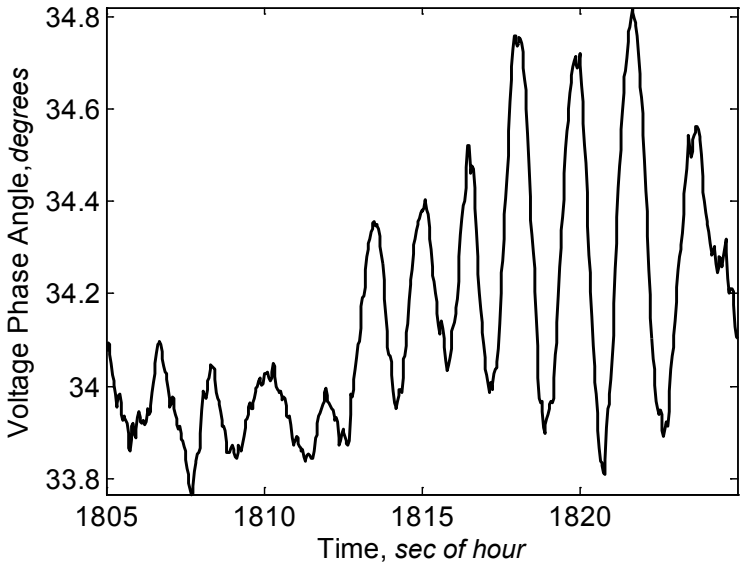

Figure 35. An example of an RPAD damped transient Event 2 (RPAD between UTPA and Waco)

In the damped transient event shown in Figure 36, the duration is 4.4 seconds and the largest swing is 0.96 degrees. The frequency of the oscillation is 0.59 Hz.

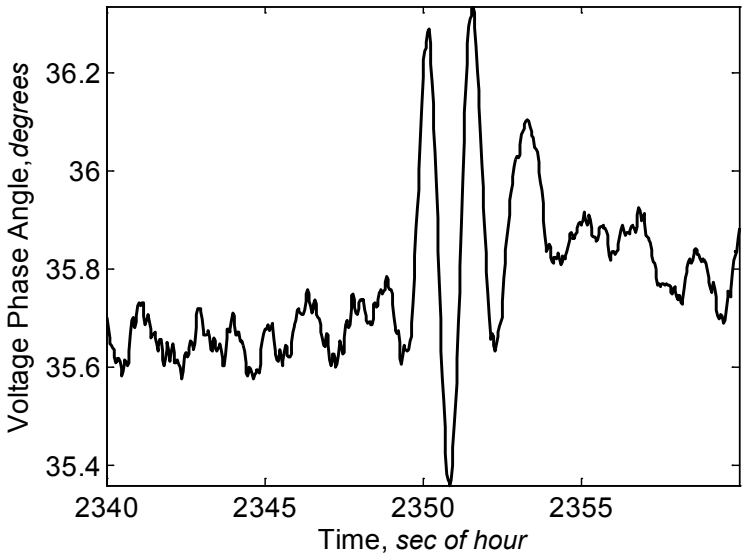

Figure 36. An example of an RPAD damped transient Event 3 (RPAD between UTPA and Waco)

The detected frequencies in the signal that are of interest fall below 2.0 Hz. This range of frequencies is typical to inter- and intra-area oscillations [6]. It is thought that the cause of the oscillation is from system modes being excited by a switching event. However, for most cases, the root cause of each switching event is unknown. One example of a sustained transient event is provided in Figure 37. For a sustained transient event in the RPAD data, the signal is not as smooth because it contains other frequencies.

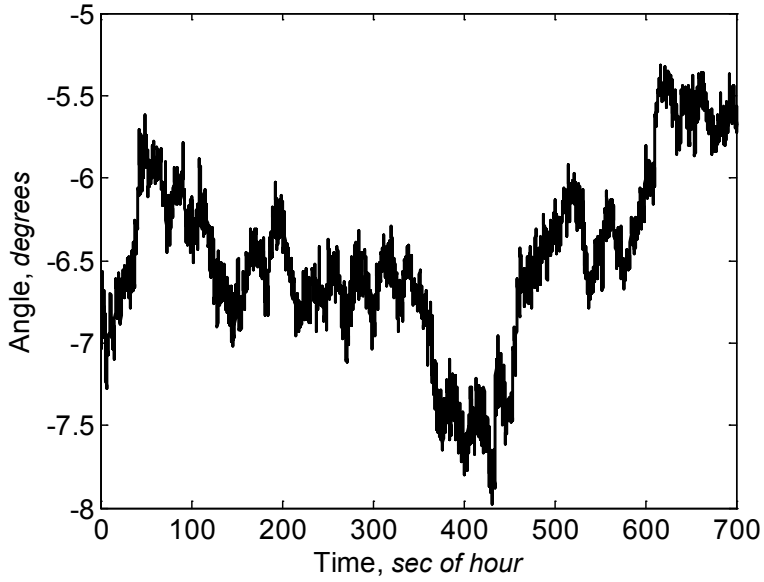

Figure 37. An example of an RPAD sustained transient (RPAD between UT-Austin and McDonald)

A detailed view of the oscillation is provided in Figure 38, where the oscillations in the voltage RPAD are clear.

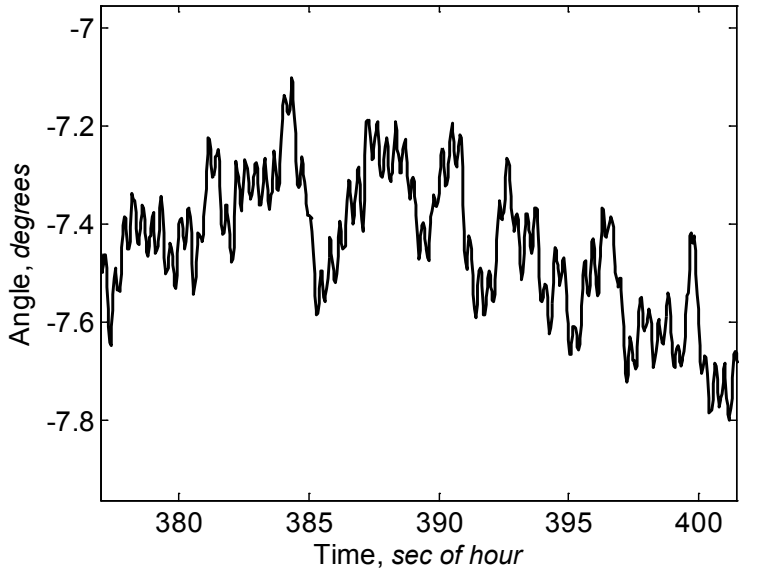

Figure 38. A detailed example of an RPAD sustained transient (RPAD between UT-Austin and McDonald)

A sustained transient event is easily identified when examining the PSD contour plot shown in Figure 39 starting at approximately 350 seconds. The frequency of this type of oscillation is approximately 2.8 Hz, higher than the frequencies seen in the damped transients shown in the previous examples.

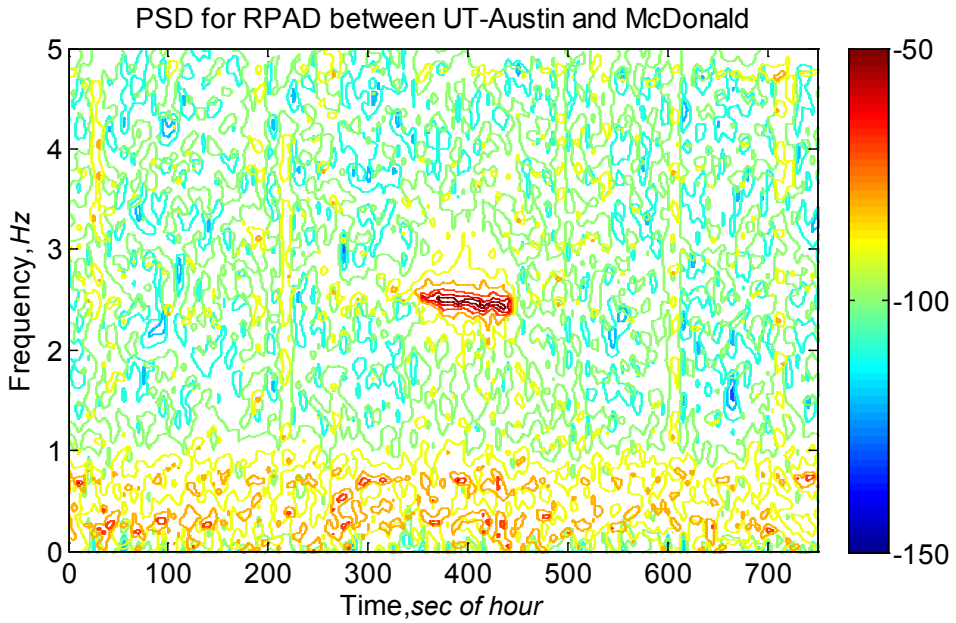

Figure 39. A contour plot of the PSD (low-frequency content over time) for a voltage RPAD sustained transient event (RPAD between UT-Austin and McDonald)

4.1.1.3 Step Change in RPAD

The following events are categorized as step changes in the RPAD data. During a step change event, the RPAD suddenly changes from one value to another lower or higher value. The direction of the change depends on the reference point from which the phase angle is measured and the effect of the change of power flow caused by the event. The change in the RPAD can vary, from less than 1 degree to up to 10 degrees or more. Large system changes in power flow, such as a generator unit trip, can result in larger step changes. Although the exact cause is unknown, it is assumed that smaller RPAD step changes are caused by transmission line trip or reclose events and larger step changes are caused by generator unit trips. The step changes in the RPAD caused by generating unit trips can be confirmed in the ERCOT Daily Grid Reports when sudden-loss-of-generation events above 450 MW are reported [3].

Transmission line trips can occur when a fault is detected on the line. A line trip causes the redirection of power to surrounding transmission lines, causing a change in the measured RPAD. When an auto-reclosing practice is utilized, breakers on both ends of the line will reclose automatically, typically after a period of 2 seconds following the initial line trip. If the fault is temporary, the line reclosing operation will likely be successful and no further protective action is needed. As a result, power will return to its original value, and the RPAD will return to its pre-fault value as well. If the fault persists, breakers will trip the line again and the reclosing operation is repeated as necessary. However, reclosing events do not normally occur more than three times. For permanent faults, the last trip operation of the sequence will result in the protected line remaining offline. Depending on the utility, voltage level, and type of line, the number of trips and reclosing actions and the wait period between the reclose and trip actions will vary [9]. Figure 40 represents a sustained step change event. For this event, the RPAD drops from

-56.53 degrees to -56.85 degrees. The ramp rate is 4.86 deg/sec. The event here appears to be caused by a transmission line trip.

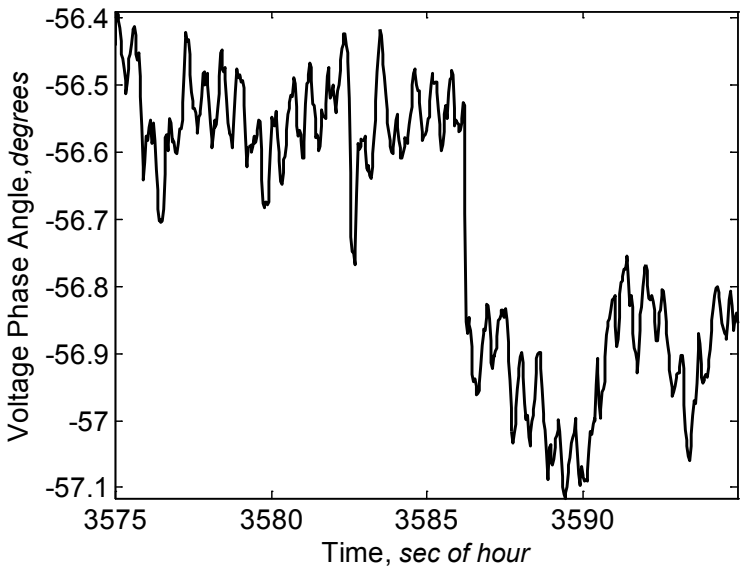

Figure 40. An example of an RPAD sustained step change event (RPAD between McDonald and Waco)

In the second event, shown in Figure 41, a momentary step change occurs. The RPAD starts at -67.39 degrees and rises to -67.13 degrees before returning to -67.45 degrees. The duration of the event is 1.23 seconds (74 cycles), the ramp-up rate is 2.57 deg/sec, and the ramp-down rate is 2.56 deg/sec. Again, because the RPAD suddenly switches to a new value and then returns to its approximate original value, it is assumed that the cause of the event is a transmission line reclose.

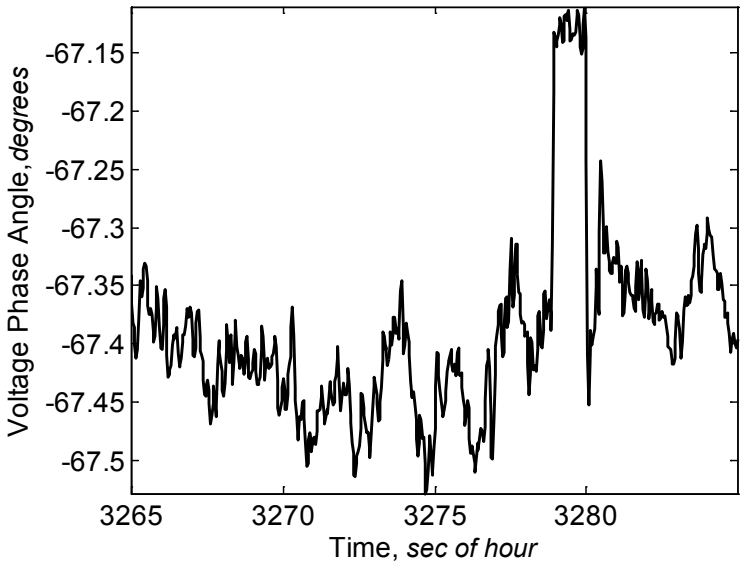

Figure 41. An example of an RPAD momentary step change event (RPAD between UT-Austin and Waco)

4.1.2 Frequency Event Categories

The event categories seen in the frequency are presented here with examples shown for each category. Although the PMU frequency is calculated using the voltage RPAD data, some events are more easily detected in the frequency signal than the RPAD signal. For example, a sudden, large imbalance in load and generation caused by a generating unit trip would cause the frequency across the entire system to drop significantly. The drop in frequency and rate of change depend on the amount of power lost and the inertia of the system. The frequency drop during a generating unit trip is of significantly greater magnitude than the frequency during normal operating conditions and can easily be detected.

Smaller systemwide imbalances in load and generation also cause sudden frequency rises and drops that are not visible in the RPAD. The frequency also shows events that are local to the PMU station and does not rely on the difference between two PMU stations such as is needed by the RPAD signals. If an event is detected in the frequency at only one PMU station and is not visible in any of the other PMU frequencies, it is likely that an event occurred near the PMU station where the event was detected. Impulse events are predominantly local events. Some transient events are local and are most likely caused by equipment or events located nearby. Local events do not indicate an imbalance in system load and generation.

4.1.2.1 Impulse

Impulse events seen in the frequency are presented here. The frequency impulse is similar to a high-frequency oscillation with duration of either one cycle or one-half of a cycle and fall into the large-impulse or small-impulse subcategories. The events occur only in the McDonald frequency data, indicating that some sort of switching event or motor starting occurs near the McDonald PMU station on either the transmission or distribution voltage level. It is possible that these types of events cause a frequency event because of a sudden difference between the local load and generation. This type of event occurs frequently and may represent a temporary imbalance in load and generation locally. Another event that could cause a local imbalance includes a sudden trip and reclose of a large load (such as a processing plant). Impulse events seen in a PMU frequency are always seen in the corresponding RPADs. The frequency signals are used to determine at which station a local event occurs. The RPAD signal cannot be used to determine where a local event occurs because two PMU measurements are involved. For example, if an impulse event is detected in the frequency at McDonald, the same impulse event is seen in the McDonald-UTAustin and McDonald-UTPA RPADs. This always occurs specifically for impulse events but is not always true for other event categories.

The first example, as shown in Figure 42, is of a “full-cycle” impulse and belongs to the large-impulse subcategory. The duration of the event is 0.47 seconds (28 “60-Hz” cycles), and the impulse magnitude is 42.3 mHz. The ramp rate from peak to peak is 253.8 mHz/sec.

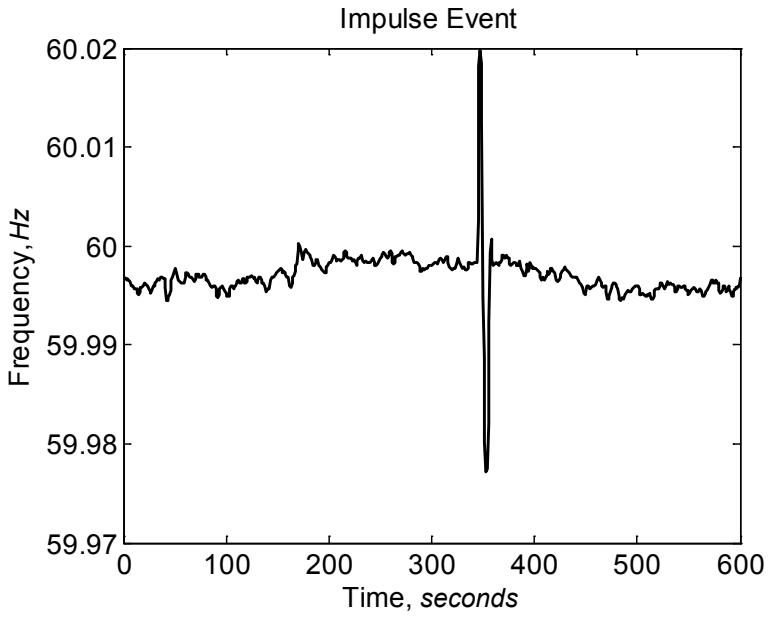

Figure 42. An example of a frequency impulse Event 1

The second example, as shown in Figure 43, is of a half-cycle impulse and belongs to the small-impulse subcategory. The duration of the event is 0.4 seconds (24 "60-Hz" cycles), and the impulse magnitude from peak to peak is 7.1 mHz. The ramp-down and -up rates are 26.43 mHz/sec and 58.87 mHz/sec.

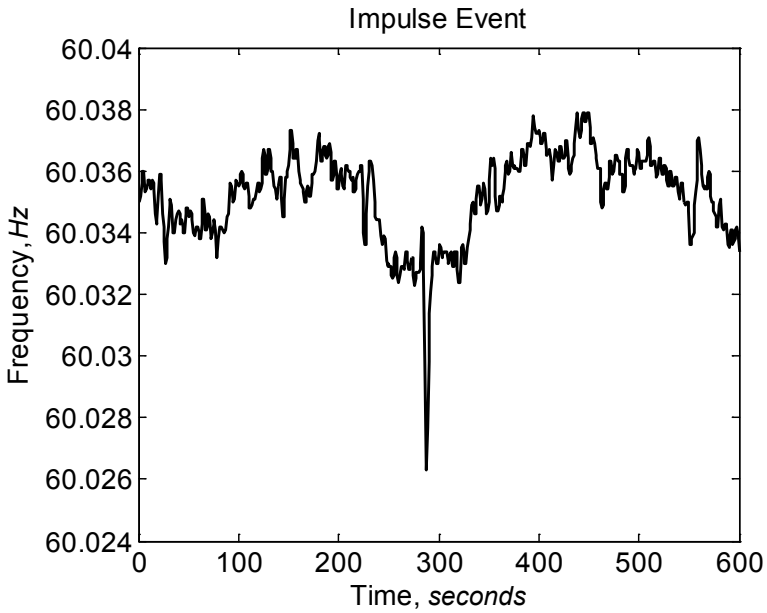

Figure 43. An example of a frequency impulse Event 2

4.1.2.2 Transient

Transient events in the frequency data are not as common as impulse events. An example of a damped oscillation is provided in Figure 44, in which the duration of the event is 5 seconds. The largest peak-to-peak amplitude during the event is 10 mHz. The frequency

of the oscillation is 1.23 Hz. The frequency of the oscillation falls within the intra-area oscillation range. Intra-area oscillations are caused by one synchronous machine oscillating against a group of machines in the area.

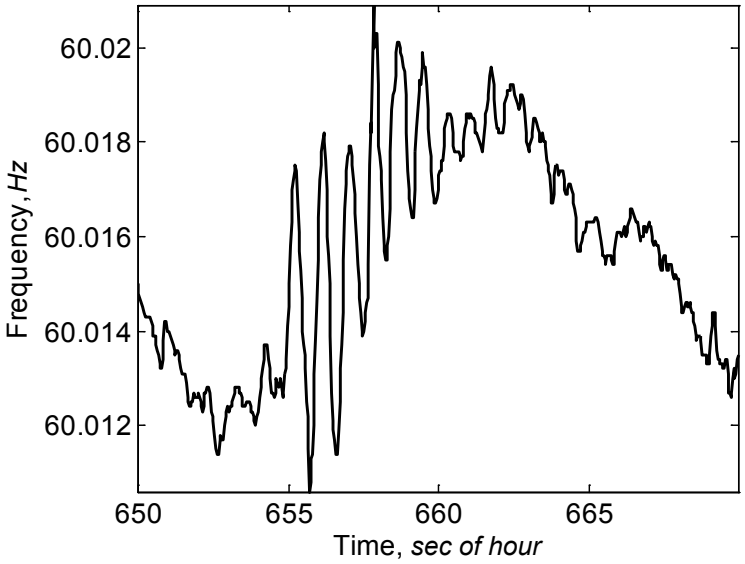

Figure 44. An example of damped transient event

An example of a sustained transient event is shown in Figure 45. The sustained transient event is detected in the UT-Austin PMU signal but is not present in the McDonald PMU signal.

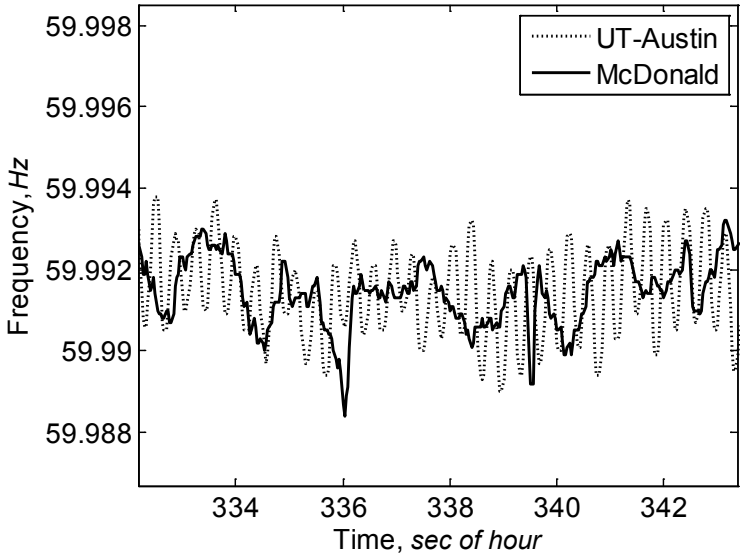

Figure 45. An example of a sustained transient event

Although it is clear in Figure 45 that the event occurs only at UT-Austin, the PSD contour plot provides a simpler way to visually detect sustained transient events,

including when the transient begins and ends and the approximate frequency of the transient. The PSD contour plot is shown in Figure 46.

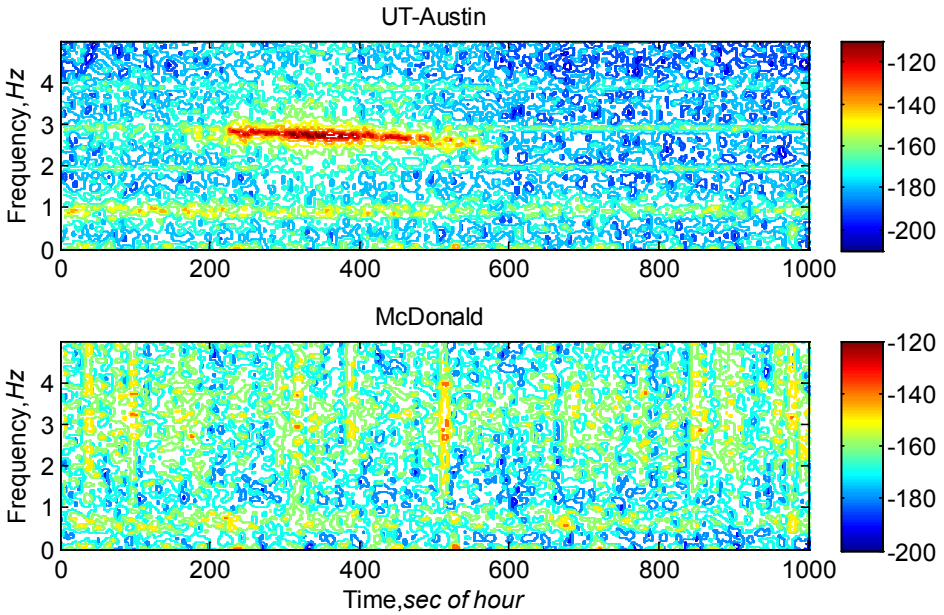

Figure 46. A contour plot of the PSD (low-frequency content over time) for a sustained-frequency transient event

4.1.2.3 Sudden Drops or Rises in Frequency

Small drops or rises caused by sudden imbalances between load and generation are detected in the PMU frequency data. These types of events are also typically detected at all PMU locations at the time of the event. An example of an imbalance caused by higher generation compared to load (the frequency increases above 60 Hz) is shown in Figure 47. The event does not have a duration, but the rate of change of frequency from the bend at the start to the peak before the frequency begins to drop is 5.22 mHz/sec, significantly slower compared to the impulse event in the frequency. This event category differs from the impulse-frequency event because these types of events occur throughout the entire system, whereas an impulse event occurs only at a single PMU location. An imbalance caused by higher load compared to generation (the frequency drops below 60 Hz) is shown in Figure 48.

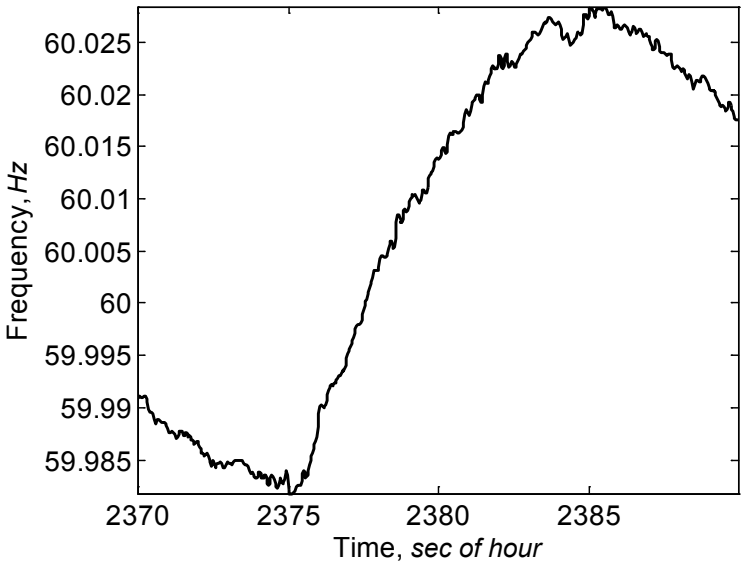

Figure 47. An example of a sudden rise in frequency

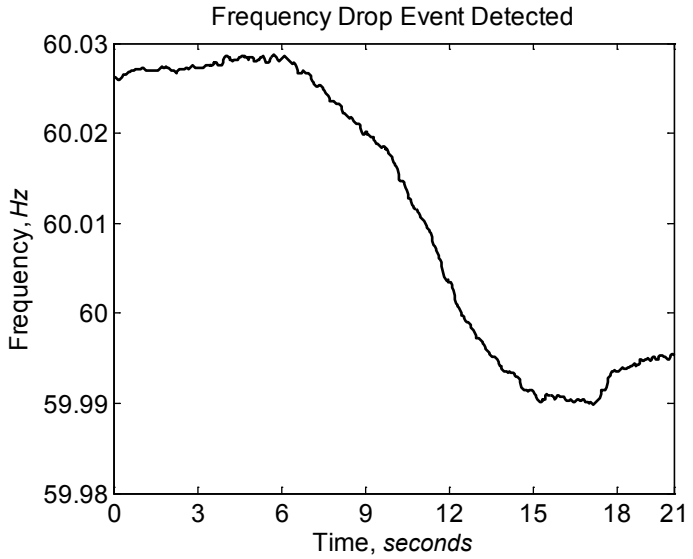

Figure 48. An example of a sudden drop in frequency

A broad view of the frequency shown in Figure 49 provides a clearer picture of how a frequency-rise or -drop event differs from normal operating conditions. During normal operating conditions, variations in the frequency are always occurring, but during a rise-in-frequency event (indicated by the red arrow), the frequency rises at a more rapid rate than is typical. Another systemwide frequency event occurs around the 1,300-second mark, when the frequency drop is of a lower magnitude (approximately 250 mHz).

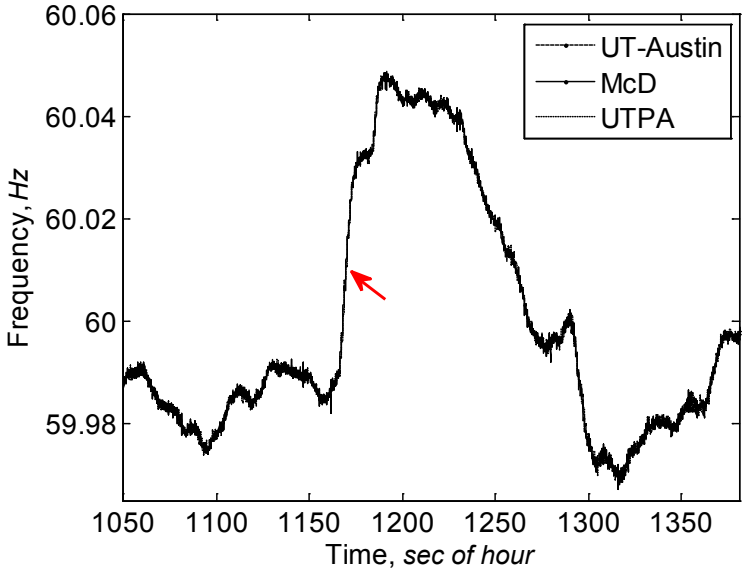

Figure 49. A systemwide frequency event seen by all PMUs

Figure 50 presents how an impulse event is a local event and is visible only at a single PMU station. The event was detected in the McDonald PMU frequency but is not present in either the UT-Austin or UTPA PMU frequencies. These examples illustrate that a PMU frequency contains systemwide information as well as local information. The variation in PMU frequencies during a large loss of generation in Section 5.2 also illustrates how the frequency differs across the power system during a drop-in-frequency event.

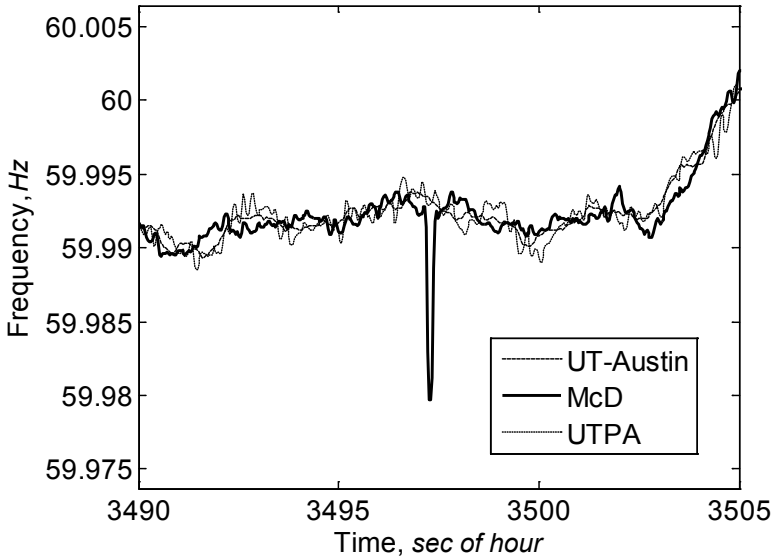

Figure 50. A local frequency event that occurs only in the McDonald PMU

5 Algorithm Development

After the events have been placed into the separate categories outlined in Section 4, the characteristics from each type of event are extracted to determine which numerical characteristics are common to each category. An algorithm is written that utilizes the common characteristics to automatically identify events. For example, if an event has a strong 0.56-Hz frequency, the event will be identified as a transient event. In this section, the RPAD categories are examined first, followed by the frequency categories. For both the RPAD and the frequency, the characteristics that are unique to each category are identified. A flowchart of the algorithm to automatically categorize events and the useful characteristics in each category is given for the RPAD and the frequency.

5.1 Extracted Characteristics for RPAD

This section examines the characteristics that are common to categories in the RPAD data described in Section 4.1. The categories are impulse, transient, and step change. The methods that are used to extract these characteristics are similar to the methods described in Section 2 and Section 3 used to screen the PMU data for events. The methods are FFT, Yule-Walker, differential of the PMU data, and matrix-pencil. The FFT and Yule-Walker methods are spectral methods used to identify strong oscillations within the PMU data. The differential of the PMU data is used to detect sudden changes in the data. The matrix-pencil method can be used to identify the damping and strength of the oscillations in the PMU data. The following subsections describe the characteristics for each category.

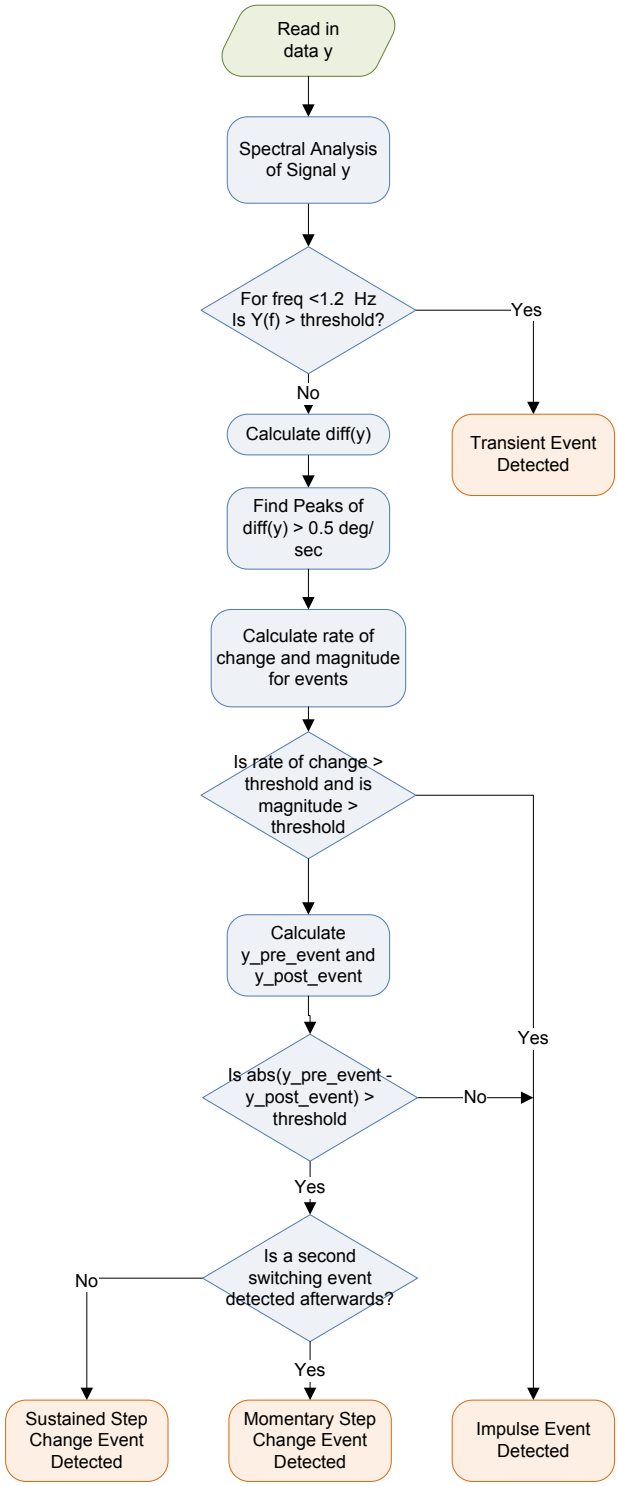

Figure 51. A flowchart for the algorithm to categorize RPAD events

The flowchart for the algorithm for the categorization of events in the RPAD data is shown in Figure 51. It is assumed that each identified event falls into at least one of the categories: sustained step change event, momentary step change event, impulse event, or transient event.

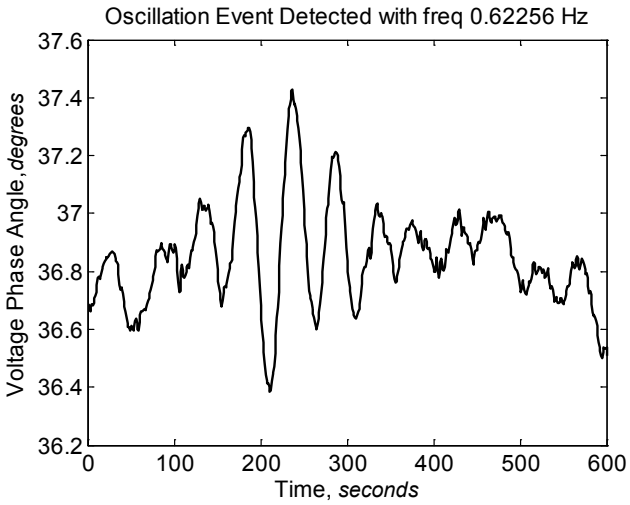

Figure 52. An example of a PMU RPAD oscillation event

Two functions are used to categorize the events based on the extracted characteristics. The first function determines if the event is a transient event by examining the peak power for frequencies below 1.2 Hz. If the detected peaks are above a selected threshold, the event is identified as a transient event. The power for an inter- or intra-area oscillation during a transient event is typically very high. To illustrate, an example of a transient event and its characteristics is provided. The detected event in the RPAD data is shown in Figure 52. The event was originally detected by the screening algorithm from Section 2 and Section 3. After the event is detected, the algorithm examines the frequency content of the signal. The Yule-Walker method is used to find the strength of the frequency content in the signal. The frequency content below 1.2 Hz is examined, and if the peak power for a frequency below 1.2 Hz is above the selected threshold, the event is identified as an oscillation event.

The Yule-Walker calculates PSD for frequencies below 1.2 Hz, as shown in Figure 53. The peak frequency of the 0.62 Hz indicated is well above the selected threshold of -80 dB. For the algorithm, the threshold is selected based on examining multiple transient events that have been detected by the screening algorithm. For comparison, the Yule-Walker calculates the PSD for a non-transient event, as shown in Figure 54. The peak dBs of frequencies of interest fall well below the -80 dB threshold.

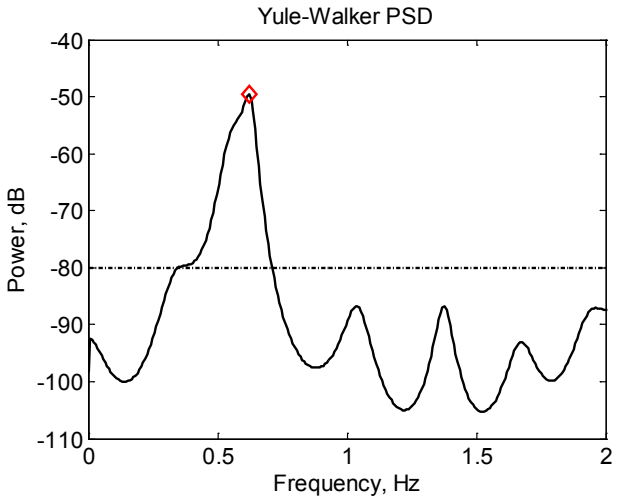

Figure 53. An example of an oscillation-event PSD

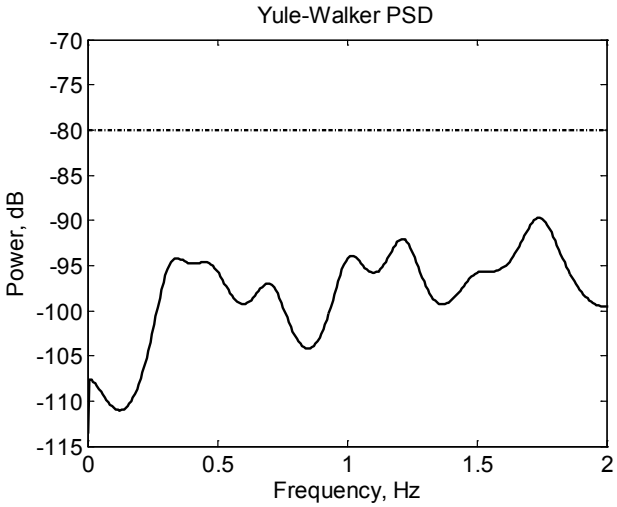

Figure 54. An example of a non-oscillation-event PSD

The second function identifies the detected event as either an impulse event, a momentary step change event, or a sustained step change event in the RPAD. The function uses the differential of the PMU RPAD signal to determine if the event is a possible step change or impulse event. The peaks in the differential of the signal are detected, and if the peaks cross a certain threshold, the event is tagged as a possible step change or impulse event and evaluated further. For the RPAD, the thresholds of the rate of change of RPAD for impulse and step change events are above 0.08 deg/sec and below −0.05 deg/sec. An example of an impulse event shown in Figure 55 illustrates how the function is able to categorize impulse events. The (left) differential in Figure 56 has two peaks with only one (indicated by a red diamond) exceeding the defined threshold. This detected peak time is marked as a possible impulse or trip event. The (right) possible event is indicated in the original plot of the data in Figure 56. At this step, the function has not yet identified the event as an impulse or step change event, but only as a possible impulse or a possible step change event.

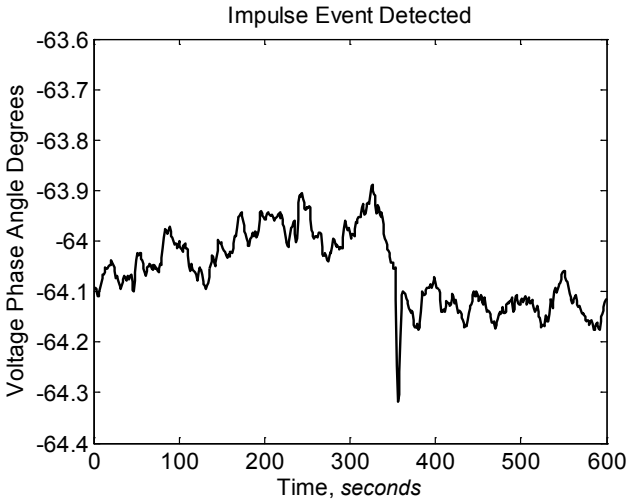

Figure 55. An event is detected in the RPAD signal

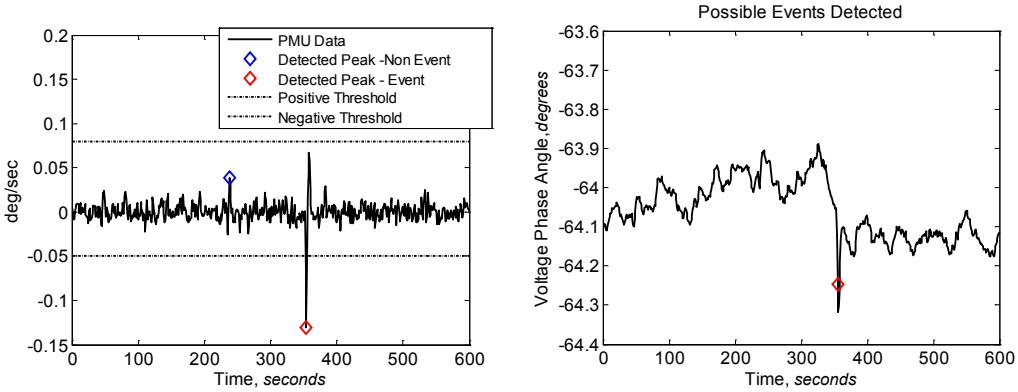

Figure 56. Methods to detect an impulse event using the differentiated RPAD signal

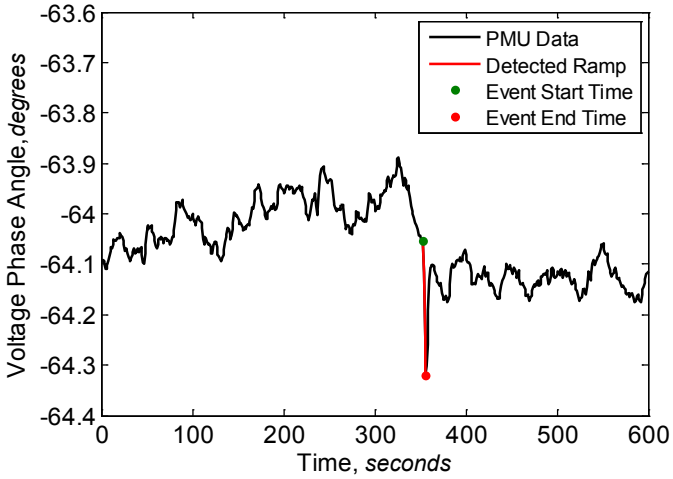

Figure 57. The start and end times and the ramping period of the detected impulse event are shown for the RPAD signal

The possible event in the original data is analyzed further to determine if the event is an impulse or a step change. The algorithm identifies the start of the ramping period and the end of the ramping period. With the starting and ending points identified, the ramp rate of the event is calculated in degrees per second. For the example event, the ramp-down rate as calculated by the algorithm is 2.66 deg/sec and is highlighted in red in Figure 57.

Next, to differentiate between step change or impulse events, the average value of 0.33 seconds (20 cycles) of the RPAD before the start point of the detected ramp, y_{pre_event}, and the average value of 0.33 seconds of RPAD after the end point of the detected ramp, y_{post_event}, are compared. This step of the algorithm is illustrated in Figure 58, in which (in green) y_{pre_event} and (in red) y_{post_event} are highlighted. If the event is a line trip, the RPAD prior to the event suddenly changes and remains at the new value. Therefore, if the difference between y_{pre_event} and y_{post_event} exceeds the selected threshold, the event is tagged as a trip event. Otherwise, the event is considered an impulse event. In the example provided, the jump falls below the selected threshold and the event is correctly identified as an impulse event by the algorithm.

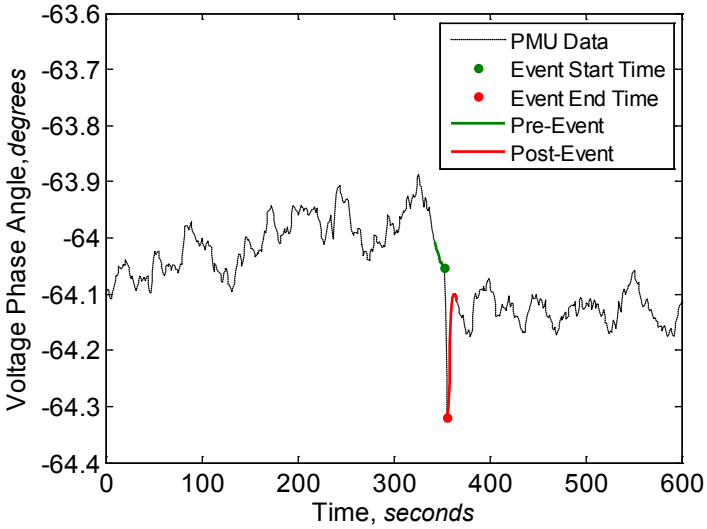

Figure 58. The (green) pre-event period and (red) post-event period are used to calculate the change in RPAD.

If the jump exceeds the threshold, the event is considered either a sustained or momentary step change event. To differentiate between sustained and momentary step change events, the number and time stamps of each detected ramp-up and ramp-down event are examined. For example, if a ramp-up time is quickly followed by a ramp-down time or vice versa, the event is tagged as a momentary step change event. If there is a single ramp-up or ramp-down event that is not an impulse, the event is a sustained step change event. Examples of a line reclose event (step) and line trip event (sustained) are shown in Figure 59.

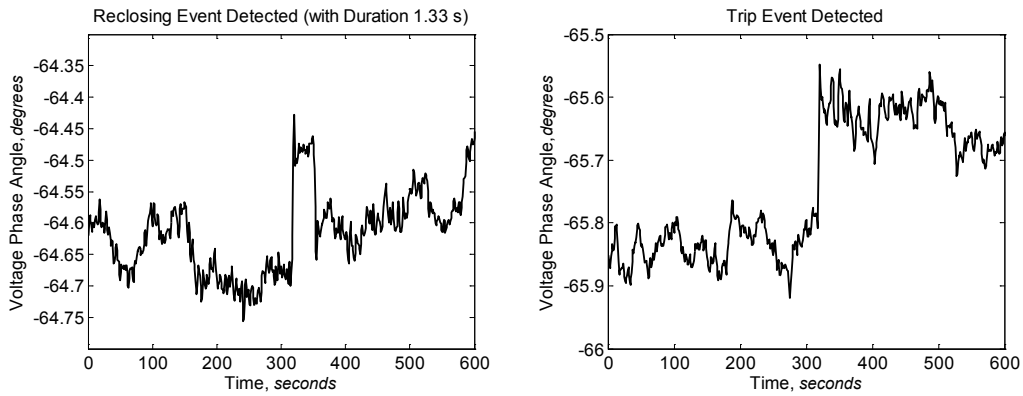

Figure 59. (Left) Examples of a momentary step change event and a (right) sustained step change event in the RPAD signal

5.1.1.1 Summary of RPAD Event Categories

After extracting common characteristics from 62 impulse events, 39 transient events, and 87 step change events, an approximate range of the event characteristics was determined. The magnitude, ramp rate, duration, frequency, and step change content of the events were extracted and saved. Note that when using the RPAD, which is the voltage phase angle between two buses separated by an unknown network, the RPAD difference indicates the strength of the effective tie line between two buses. It also shows the measure of stability of power systems. A large value of RPAD indicates a weaker tie between the two areas. Table 5 summarizes available characteristics for each category.

Table 5. Summary of Characteristics From Events Detected in RPAD Data

Category	Subcategory	*Magnitude (deg)*	*Ramp Rate (deg/sec)*	*Duration (sec)*	*Frequency (Hz)*	*Step Change (deg)*
Impulse	**Single (Small)**	0.18–0.4	0.5–5.5	0.167–0.5	-	-
	Single (Large)	1.4–1.7	7.0–16.0	0.167–0.5	-	-
Transient	**Damped**	0.15–1.5	-	<9	0.4–1.1	-
	Sustained	0.1–1.6	-	>9	0.8–3.0	-
Phase Angle Change	**Momentary (Small)**	-	0.75–3.25	0.5–1.5	-	0.2–0.6
	Momentary (Large)	-	2–10	0.5–1.5	-	0.95–1.15
	Sustained	-	1–5	-	-	0.15–0.75

5.2 Extracted Characteristics for Frequency Data

A different algorithm is used for categorizing events in the PMU frequency data. The algorithm is similar to the algorithm used to categorize events in the RPAD data, with changes made to include events only present in the frequency signal and to create new threshold values because fluctuations in frequency are smaller than fluctuations in RPAD. The category for events present only in the frequency is the sudden rise or drop in frequency. Step change events are not included because these types of events are present in the RPAD only.

A flowchart for the frequency categorizing method is shown in Figure 60. The signal is examined by all functions because it is possible for an event to belong to multiple categories. The flowchart below shows how each of the tags for the three categories is decided. After the tags have been assigned, they are examined to determine the category or categories in which the event belongs.

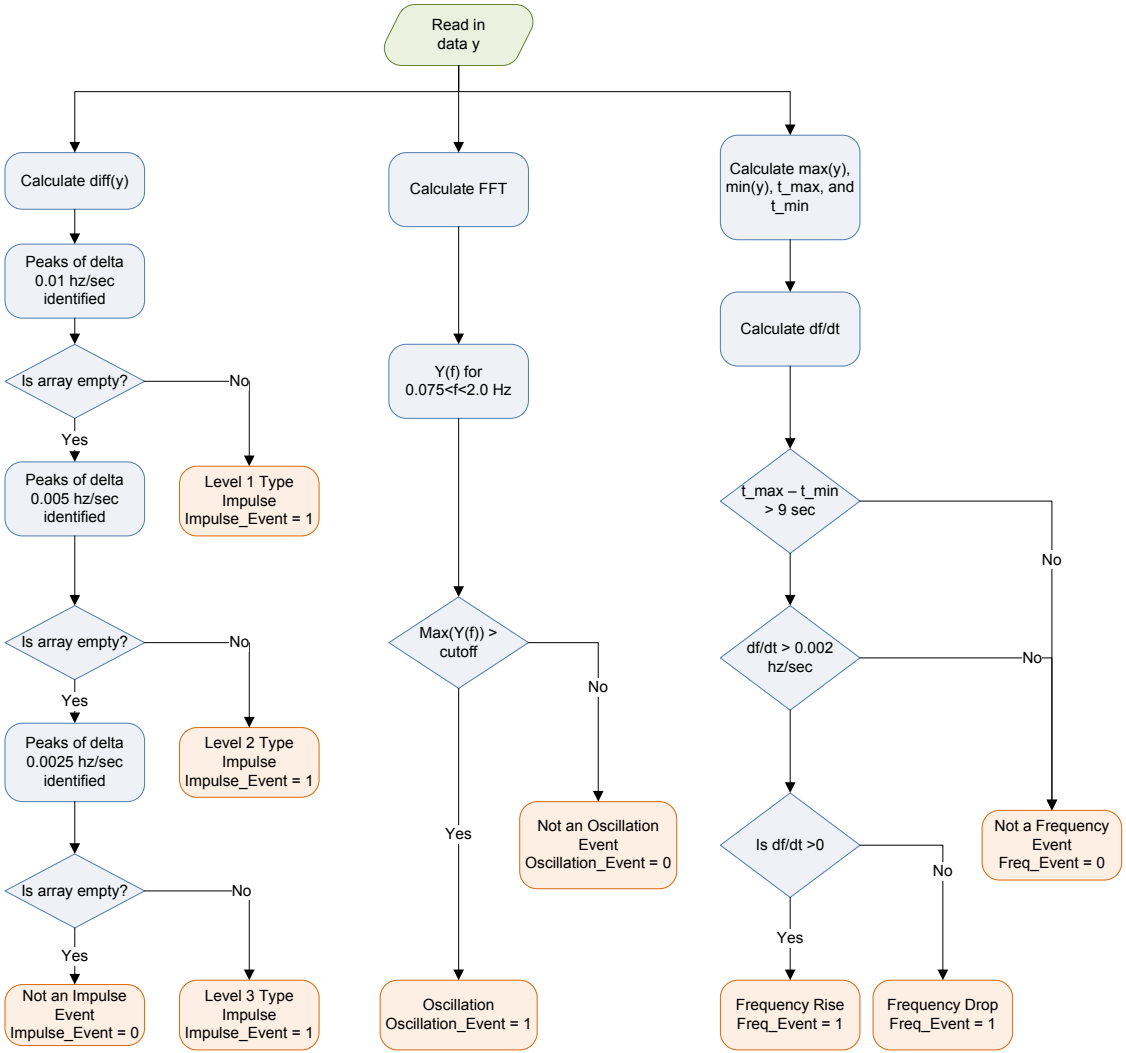

Figure 60. A flowchart for the algorithm to categorize frequency events

In this section, examples of the events and the analysis used to identify the events are given. The first category that is examined is for impulse events, which can fall into two different subcategories. The next event category is for transient events. The third event category is a rise or drop in frequency. For the first category, in which possible impulse events are identified, the differential of the PMU frequency signal is used. Peaks in the differential are identified at three different levels. The first level is for impulses with the highest magnitude. An example of the impulse in the frequency data is shown below in Figure 61. This type of event is only found at the McDonald PMU station and could be caused by equipment on the distribution side located near the station. For the first level, the peaks in the differential of the signal are identified when previous values exceed 0.01 Hz/sec. An example of the peaks identified for the impulse event is shown in Figure 61.

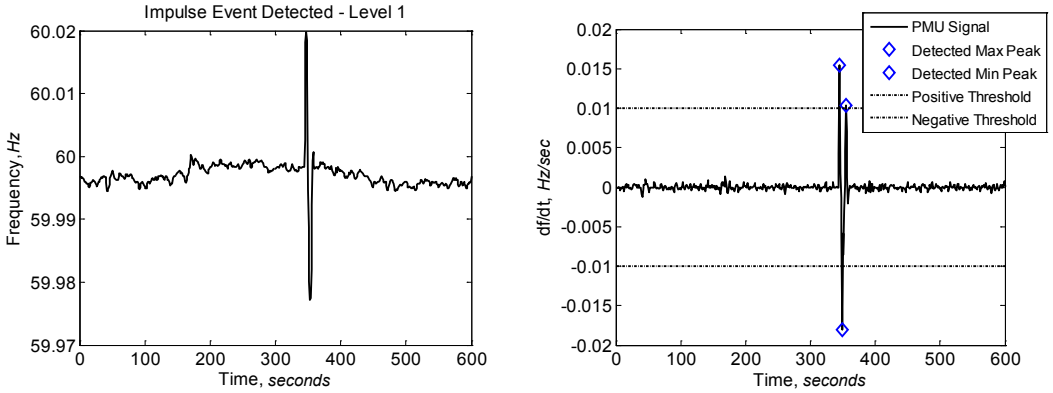

Figure 61. (Left) The impulse event and (right) the differential of the signal exceeds the selected thresholds, indicating a Level 1 impulse event is detected.

The next step is to determine if the detected peaks exceed the selected threshold values. In the case below, all the detected peaks exceed the threshold. Examples of Level 2 and Level 3 impulse events are provided in Figure 62 and Figure 63, respectively. The peak detection and threshold values are different for all impulse event levels. The first event level is an example of the large-impulse-event subcategory. The second and third levels are examples of the small-impulse-event subcategory.

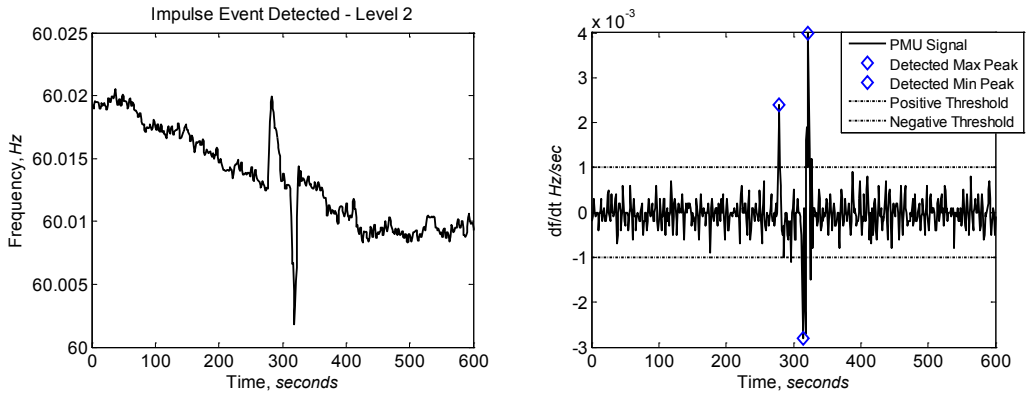

Figure 62. (Left) The impulse event and (right) the differential of the signal exceeds the selected thresholds, indicating a Level 2 impulse event is detected.

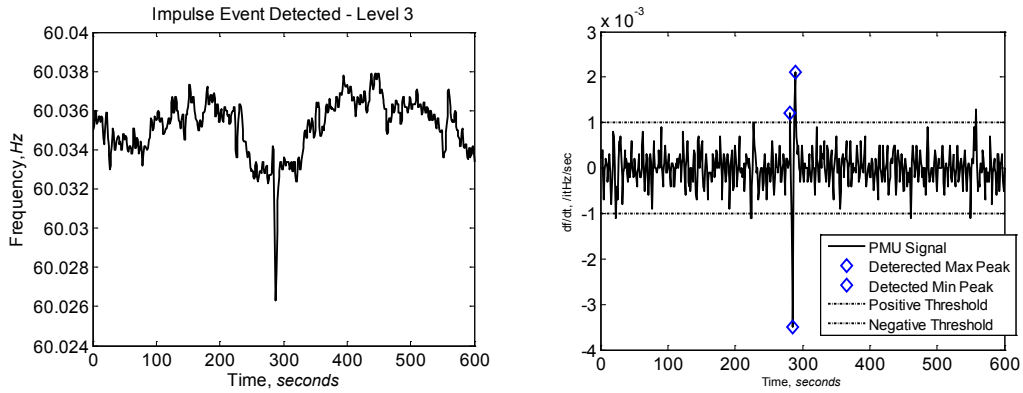

Figure 63. (Left) The impulse event and (right) the differential of the signal exceeds the selected thresholds, indicating a Level 3 impulse event is detected.

The next category that is analyzed is a transient event. The FFT of the PMU frequency signal is used to detect transient events. Transient events are typically excited by the switching of either equipment in the power system or of load or generation. Because of the structure of the power system network, the damped transient events of interest that are excited fall into the range of frequencies below 2.0 Hz. From examining the PMU data, frequencies above 2.0 Hz are present, but the cause and origin of these oscillations are not well understood at this time. These frequencies may be examined in future work and help categorize power system events further. An example of a transient event is shown in Figure 64 below. The FFT as applied to the differential of the frequency (to remove dc offset) is given as well. The peaks are detected in the 0.05- to 2.0-Hz frequency range, and if the peaks fall above the selected threshold, the algorithm assigns a transient event tag.

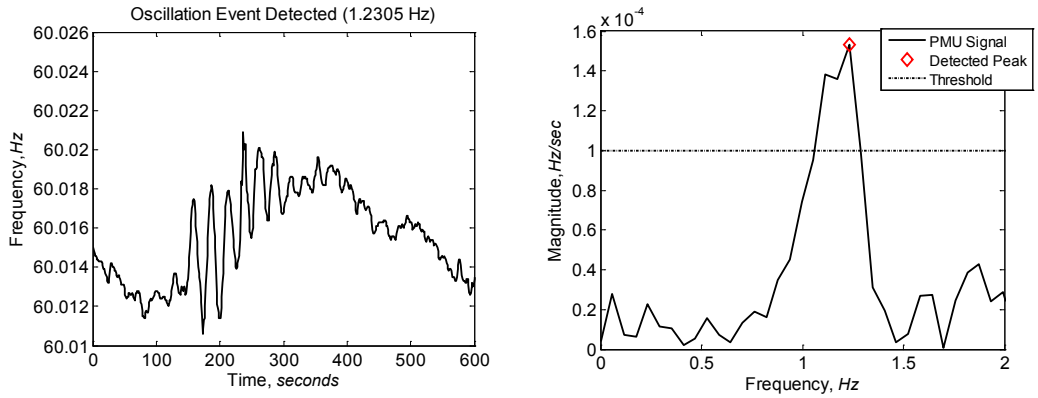

Figure 64. (Left) An oscillation event and (right) the spectral analysis showing that the frequency content for the signal exceeds the threshold, indicating a detected event.

To illustrate the difficulty of visually screening PMU data for oscillation events, a broad view of the plot of the frequency containing the event during a period of 400 seconds is shown in Figure 65. The event starts at 255 seconds.

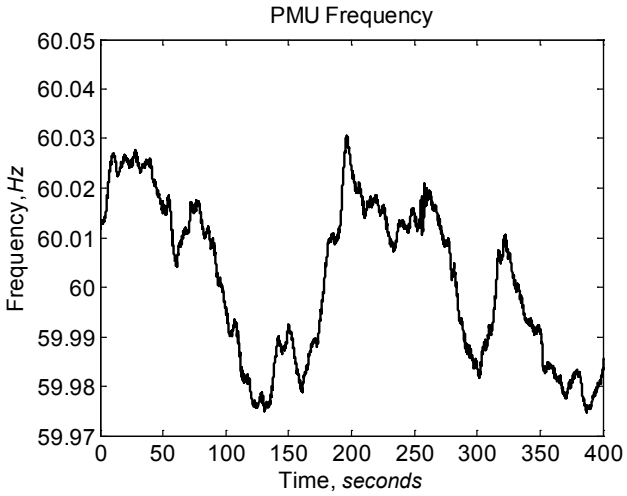

Figure 65. From a 400-second window of frequency data, it is difficult to visually detect events.

Next, to determine if the event is a rise or drop in frequency, the maximum and minimum values and the times at which these occur within a 20-second window are extracted. The time between the maximum and minimum values is calculated as well as the slope between the maximum and minimum. The first step examines if the time difference is greater than 9 seconds. This step eliminates events in which there are sudden, large changes in the signal, such as those that occur during impulse events. Next, if the slope is greater than 2 mHz/sec, the event is placed in the rise- or drop-in-frequency category. If the slope is too gradual, the event is most likely not a rise- or drop-in-frequency event. The sign of the slope is used to determine if the event belongs to a rise-in-frequency or a drop-in-frequency subcategory. If the event is a rise-in-frequency event, the frequency increases and the slope is positive. If the event is a drop-in-frequency event, the frequency decreases and the slope is negative. Examples of both types of events are provided in Figure 66 and Figure 67. The rises and drops presented in this section are from small, sudden imbalances between load and generation.

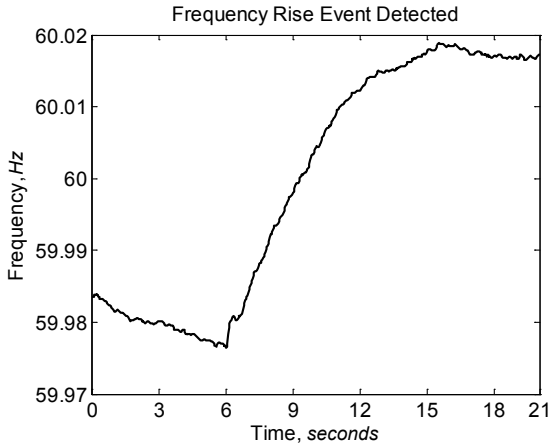

Figure 66. An example of a frequency-rise event

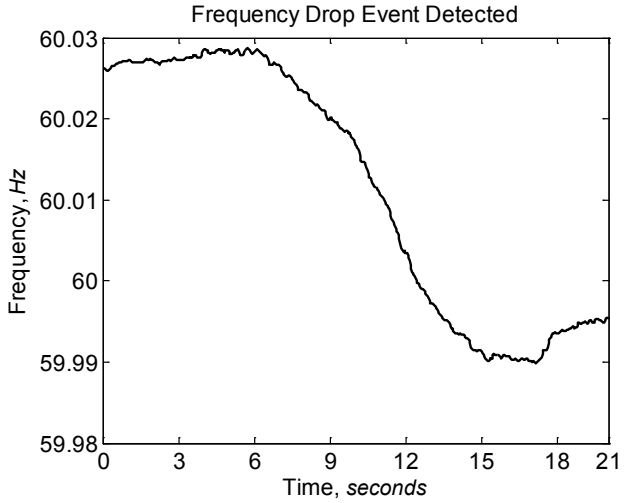

Figure 67. An example of a frequency-drop event

An example of a drop-in-frequency event is provided in Figure 68, when a sudden loss of large generation of 478 MW on January 25, 2012 at 7:13 UTC occurs.

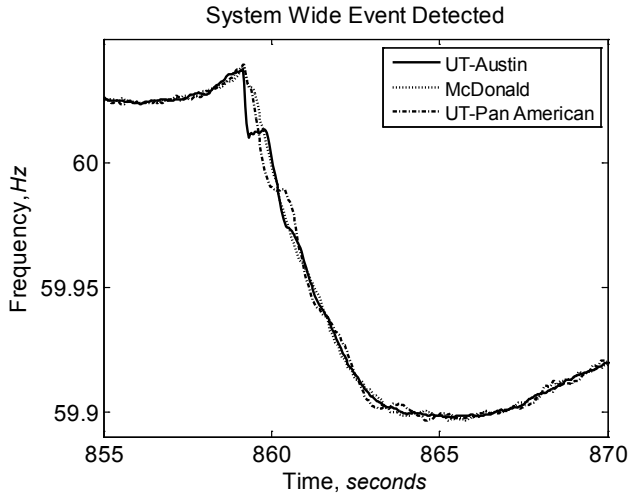

Figure 68. Another example of a frequency-drop event, on January 25, 2012, 7:13 UTC

The event was detected at all PMUs in operation at the time of the event. The frequency at the time of the event is shown in Figure 68. A more-detailed view in Figure 69 shows the initial rate of change of frequency is much higher at UT-Austin, and the frequency begins to oscillate against the frequency at UT-Pan American. The initial rate of change of frequency is approximate 300 mHz/sec, and eventually the rate of change of frequency changes to approximately 22.4 mHz/sec (from the start of the event to the nadir). A detailed view of the beginning of the event is also shown in Figure 70. The frequency at UT-Austin begins to drop before the other frequencies at the other PMU locations. The rate of change of frequency characteristic taken for unit trip events is measured by taking the frequency and time at the start of the event and the frequency and time at the minimum nadir of the event.

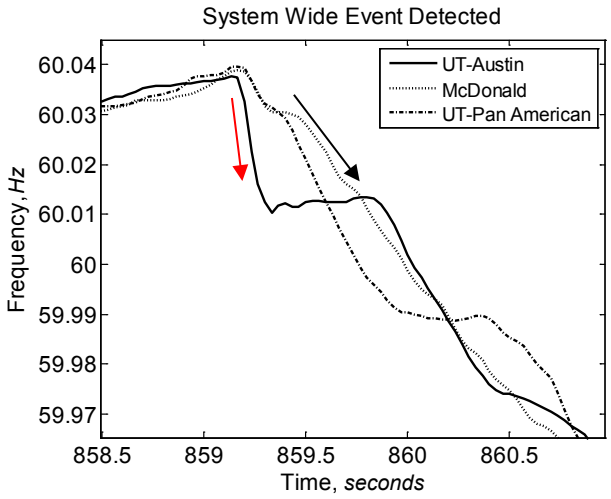

Figure 69. A detailed view of the frequency-drop event shows the rapid drop in frequency at UT-Austin and the oscillations at UT-Austin and UT-Pan American.

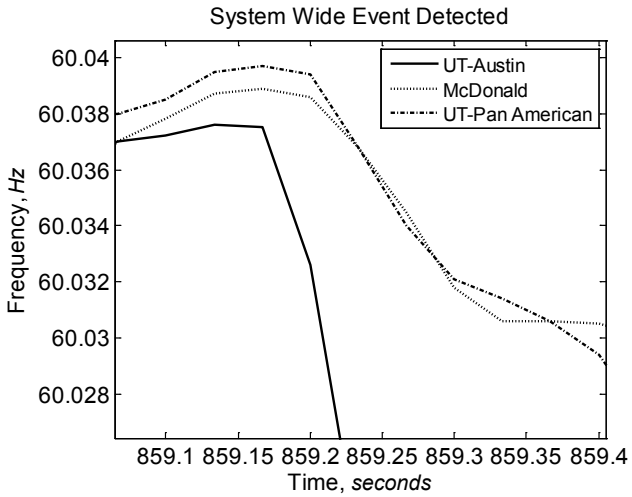

Figure 70. The frequencies at each location begin to drop at different times, with UT-Austin dropping sooner and more rapidly.

The event is also tagged as an oscillation event in the UT-Austin (1.17 Hz) and UT-Pan American (0.70 Hz) frequency data. The events are also categorized as impulse events because of sudden changes in the frequency.

5.2.1.1 Summary of Frequency Event Categories

After extracting common characteristics from 82 impulse events, 35 transient events, and 93 rise or drop events, an approximate range for characteristics of these event categories was determined. The magnitude, ramp rates, duration, frequency content, and change in frequency of the events were extracted and saved. Table 6 summarizes available characteristics for each category.

Table 6. Summary of Characteristics from Events Detected in Frequency Data

Category	*Subcategory*	Magnitude (mHz)	Magnitude Peak to Peak (mHz)	Ramp Rate (mHz/sec)	Ramp Rate Peak to Peak (mHz/sec)	Duration (sec)	Freq. (Hz)	Delta Freq. (Hz)
Impulse	Single	3–9	-	10–900	-	0.267–0.5	-	-
	Multiple	20–25, 3–10	40–50	25–250	250–500	0.3–0.6333	-	-
Transient	Damped	5–325	-	-	-	0.4–7	0.3–5.0	-
	Sustained	0.1–1.6	-	-	-	>9	0.8–3.0	-
Rise or Drop in Frequency	Rise	-	-	0.8–3	-	-	-	0.015–0.04
	Drop	-	-	2–8	-	-	-	0.02–0.1
	Unit Trip	-	-	15–30	-	-	-	0.1–0.21

6 Influence of Wind Power on PMU Measurements

In this section, the relationship between wind power penetration levels and the voltage RPAD are examined. Initial observations, after estimates of modal content in PMU data are made, are that there is correlation between wind power penetration levels and the appearance of an approximately 2-Hz mode (strongest at McDonald, but visible throughout the system) [10] [11]. These observations were first made near the beginning of the synchrophasor network's initiation (in early 2009). After examining many days of PMU and wind data, it was observed that a pattern of tightly clustered modes around 2 Hz appears during high-wind scenarios prior to approximately mid-2009. However, the pattern of tightly clustered modes around 2 Hz began to change in late 2009 and early 2010. The typical behavior from early 2009 is compared to typical behavior seen in early 2010 to the present. The linear relationship between the voltage RPAD and wind power penetration is also explored. Even though the weak relationship between power transfer and the voltage RPAD across large distances was discussed previously in Section 1, the power transfer from wind power plants in West Texas to major load centers in Central Texas has a strong linear relationship to the measured voltage RPAD between McDonald (West Texas) and UT-Austin (Central Texas). In this section, examples of the relationship between wind power and the modal frequency in the PMU data are provided. However, after examining PMU data taken in late 2009 to early 2012, the relationship between the strength of the 2-Hz modal frequency and wind power penetration levels in the latter years is weak or nonexistent. Examples are provided to show how the relationship between wind power penetration and modal frequency has changed over time. In this section, the ERCOT wind power data and its linear relationship to the voltage RPAD data is examined in Section 6.1. The impact of wind power on modal frequency estimates extracted from the PMU data are examined in Section 6.2.

6.1 ERCOT Wind Power Data and Relationship to Voltage RAPD

Wind power and generation data required for this research was captured from the ERCOT website (no longer available) from January 27, 2009, to November 6, 2010. The data on the website included the aggregate wind power, aggregate generation, aggregate load, system frequency, and zonal pricing (before ERCOT switched to nodal pricing) and was updated at one-minute intervals. The time stamp for this data employs Central Standard Time and is not synchronized with the global positioning system time stamp used to time stamp the PMU data. The collected data also has a lot of missing data points. Gaps range from a few hours in a day to months' worth of missing data. Aggregate wind power and generation are now available online as hourly averages in PDF format. The resolution of this data is too low for thorough analysis.

An example of one day of wind power and wind power penetration is provided in Figure 71. The left y-axis corresponds to the wind power (MW) and the right y-axis corresponds to the wind power penetration (%). The wind power penetration within ERCOT is calculated using the aggregate wind power and total generation data. The time stamp is converted to UTC to match the PMU data time stamp for easy comparison to PMU data. During the date of the examples provided, the Central Standard Time conversion is

UTC – 5. For example, in Figure 71, the peak wind power of 4,330 MW occurs at 05:00 UTC or at 00:00 CST.

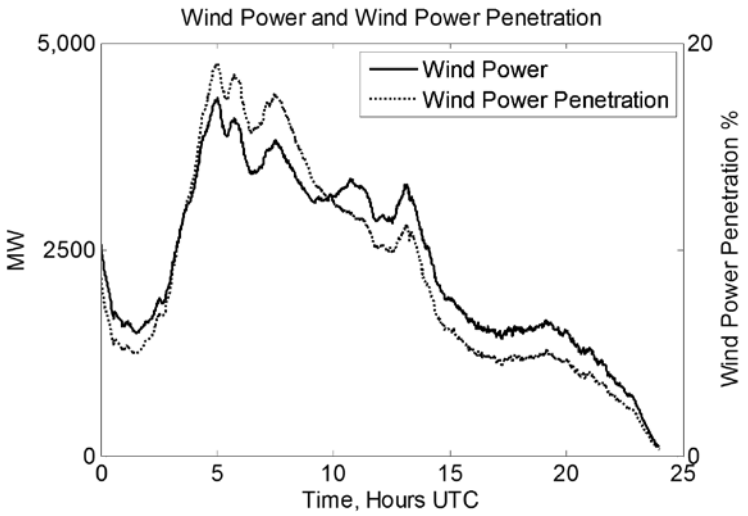

Figure 71. Aggregate wind power and wind power penetration within ERCOT on April 13, 2009 (UTC)

Initial observations also show that during higher levels of wind power penetration, the voltage RPAD between UT-Austin and McDonald is closely correlated to the wind power penetration, as shown in Figure 72. This information reveals that the voltage PMU data can be used to study power flows over a large system.

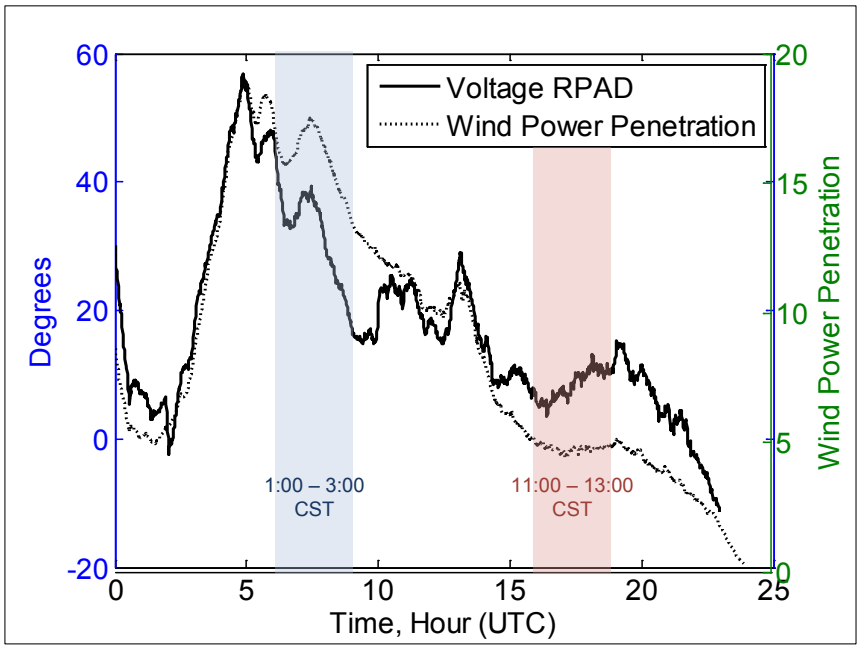

Figure 72. Voltage RPAD and wind power penetration on April 13, 2009

The highlighted areas in Figure 72. Voltage RPAD and wind power penetration on April 13, 2009Figure 72 show the periods of data to be evaluated for dynamic modal behavior

in Section 6.2. The time stamp converted to equivalent Central Time are provided for convenience as well. The blue highlighted area is the wind power penetration and voltage RPAD during a period of high wind and occurs at 1:00 to 3:00 Central Time (1:00 to 3:00 AM). The time at which high wind penetration occurs during spring within Texas typically occurs late at night to the early hours of the morning. This is when the power output from wind power plants is highest and total generation in the system is lowest. The red highlighted area is the wind power penetration and voltage RPAD during a period of low wind and occurs at 11:00 to 13:00 Central Time (11:00 AM to 1:00 PM).

6.2 PMU Signal Mode Estimates

The modal frequency and damping of low-frequency oscillations in the PMU data are made using the auto-regressive parameter estimation using the Yule-Walker method, available in the Matlab Signal Processing Toolbox [5]. The number of modes estimated is set to 32, but only modes with frequency under 3 Hz are examined in this section. Estimates are made for a moving window of 5 minutes of PMU data. The estimates from each window are saved and plotted over a period of 2 hours. The frequency estimates, plotted on the y-axis, and the damping ratio estimates, plotted on the x-axis, made during a period of low wind power penetration is provided in Figure 73. The data used for the analysis is the data highlighted in red in Figure 72. The estimates are made using data from 16:00 to 18:00 UTC (11:00 to 13:00 Central Time) when the wind power penetration is between 4.6% and 5%. The wind power during this time period is between 1,500 and 1,620 MW. There are clusters around the 1-Hz and 0.5-Hz modes that are always present. Other modes are present from 1.5 Hz to 3 Hz but are not as tightly clustered. This type of pattern occurs during time periods when the wind power penetration levels are low during the early months of 2009.

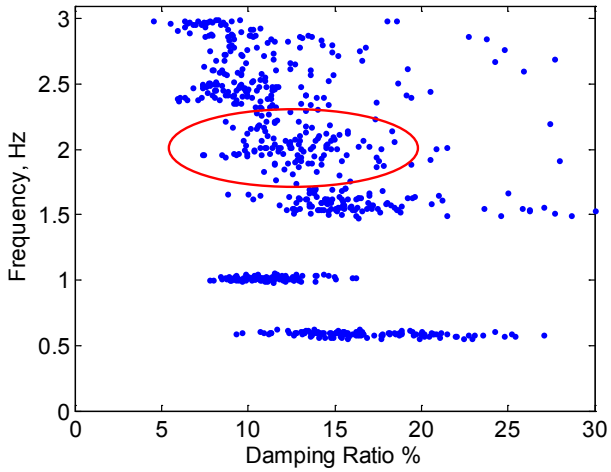

Figure 73. Modal frequency and damping estimates for low-wind conditions on April 13, 2009

A time period of high wind power penetration is examined. The data used for the analysis is the data highlighted in blue in Figure 72. The data time period is from 6:00 to 8:00 UTC (1:00 to 3:00 Central Time) when the wind power penetration is between 15% and 18%. The wind power during this time period is between 3,425 and 3,940 MW. The same

clusters around 1 Hz and 0.5 Hz are present; however, the modes around 2 Hz and 1.5 Hz are more tightly clustered. This pattern is seen during periods of high wind in early 2009.

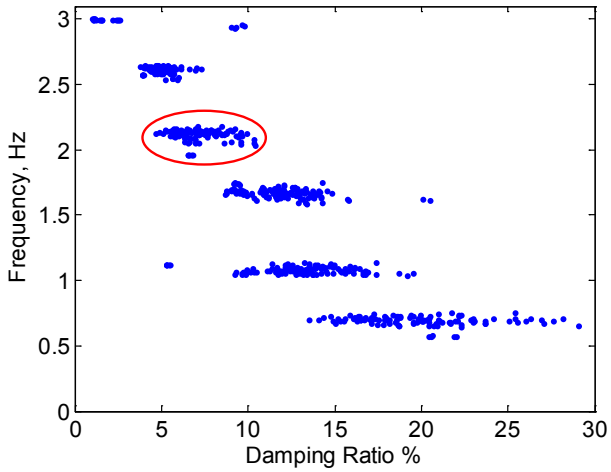

Figure 74. Modal frequency and damping estimates for high-wind conditions on April 13, 2009

It is observed that this pattern of tightly clustered modes of 2 Hz during high-wind scenarios began to change in late 2009 and early 2010. To illustrate this, a day with a similar wind profile was found in early 2010. The wind penetration and voltage RPAD between UT-Austin and McDonald are shown in Figure 75. The wind power penetration and the voltage RPAD follow each other closely, especially during sudden ramping periods in wind power.

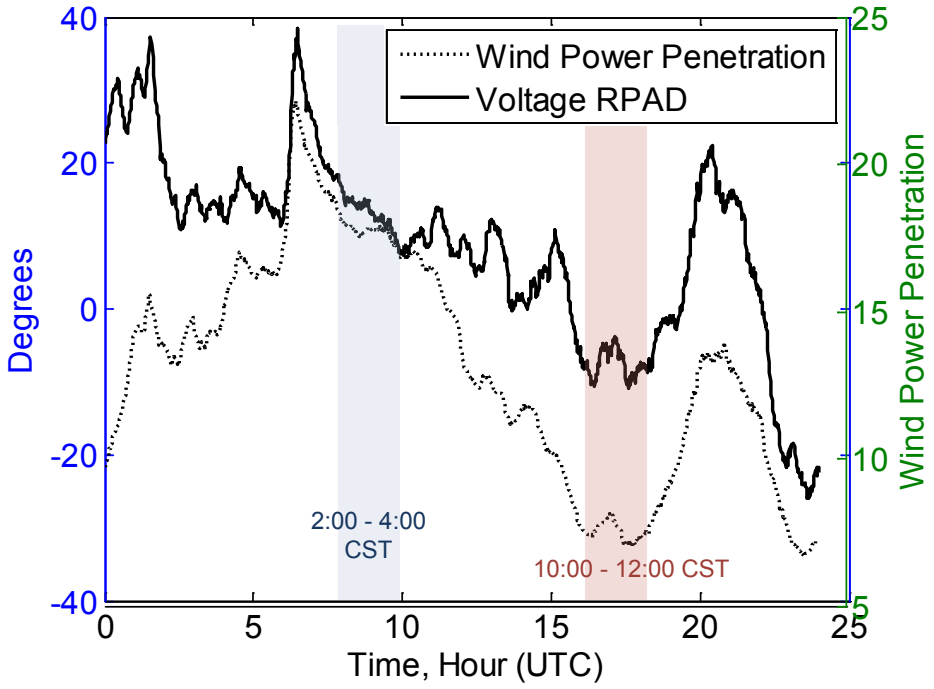

Figure 75. Voltage RPAD and wind power penetration on January 18, 2010

The highlighted areas in Figure 72. Voltage RPAD and wind power penetration on April 13, 2009Figure 75 show the periods of data to be evaluated for dynamic modal behavior. The time stamp converted to equivalent Central Time are provided for convenience as well. The blue highlighted area is the wind power penetration and voltage RPAD during a period of high wind and occurs at 2:00 to 4:00 Central Time (2:00 to 4:00 AM). The red highlighted area is the wind power penetration and voltage RPAD during a period of low wind and occurs at 10:00 to 12:00 Central Time (10:00 AM to 12:00 PM).

The frequency and damping estimates in the voltage RPAD are saved for a period of two hours during high wind power penetration. The data is taken from 8:00 to 10:00 UTC and the wind power penetration during this period is between 16.8% and 18%. The wind power during this time period is between 4,575 and 4,830 MW. However, in this case the frequency estimates are not as tightly clustered around 2 Hz as during the April 2009 case. Multiple days of data are examined to show that the relationship between the wind power and the clustering of the approximate 2-Hz mode is not as strong as would be expected from analysis of mid-2009 data.

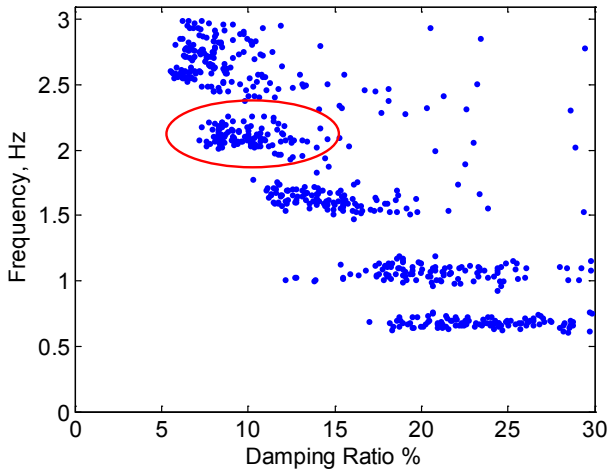

Figure 76. Modal frequency and damping estimates for high-wind conditions on January 18, 2010

Modal frequency and damping estimates are also made for a period of the same day when the wind power output is low, as shown in Figure 77. The data is taken from 16:00 to 18:00 UTC, and the wind power penetration during this period is between 7% and 7.8%. The wind power during this time period is between 2,275 MW and 2,625 MW. However, the approximate 2-Hz data is tightly clustered, which is the opposite of what occurred in the April 2009 case.

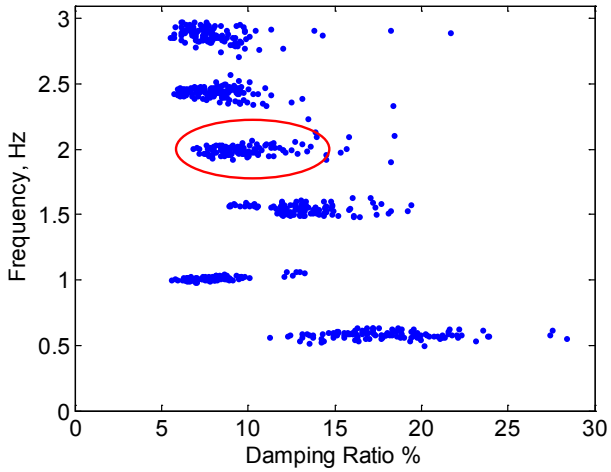

Figure 77. Modal frequency and damping estimates for low-wind conditions on January 18, 2010. The 2-Hz oscillations are still present, even though the wind penetration levels were low.

The two cases provided above show that the relationship between frequencies present in the PMU data and wind power penetration has changed over time. Possible reasons for these changes may include new transmission in wind-rich resource areas, new wind plants or conventional generators coming online, retirement of old generators, or other significant system changes. An annual report on the Electric Systems Constraints and Needs released at the end of December in 2010 includes a summary of major completed

transmission improvements [12]. In the summary is a list of improvements made in 2009 and 2010, including some two-line rebuilds and a new autotransformer all located in West Texas. The same report for the following year shows upgrades to transmission lines in the northwest region of ERCOT that could also have an impact on the dynamic modal behavior of the system [13]. A few more examples of estimated modes during high wind power penetration are provided in Figure 78 to Figure 82 to illustrate that the cluster of modal estimates around 2 Hz is not always present.

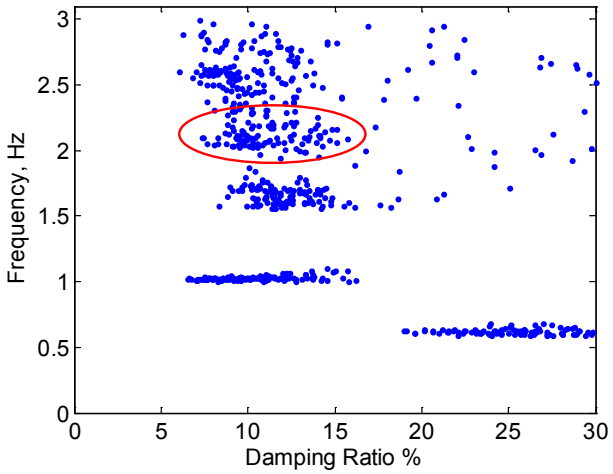

Figure 78. Modal frequency and damping estimates for high-wind conditions on January 27, 2012, 9:00 to 11:00 UTC

In Figure 78, the wind power output during the duration of the analysis on January 27, 2012, was 6,000 MW to 6,500 MW, and the wind power penetration was above 20% during this period. The wind data taken starting in August 2010 to the present can be found in ERCOT Wind Integration Reports [14]. The data was taken from 3:00 to 5:00 Central Time or 9:00 to 11:00 UTC. The approximate 2-Hz mode at this time is spread out along both the y-axis and the x-axis, consistent with observations made that during high-wind conditions, the modal estimates do not cluster tightly around 2 Hz.

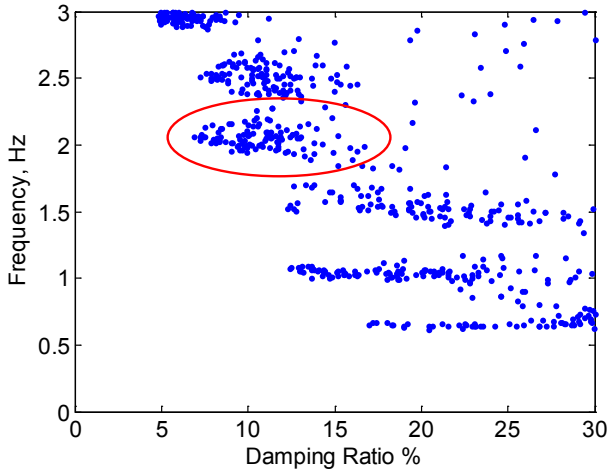

Figure 79. Modal frequency and damping estimates for high-wind conditions on November 8, 2010, from 4:00 to 6:00 UTC

In Figure 79, the wind power output during the duration of the analysis on November 8, 2010, was approximately 6,000 MW, and the wind power penetration was approximately 20%. The data was taken from 22:00 to 00:00 November 7, 2010, Central Time or 4:00 to 6:00 November 8, 2010 UTC. The modal estimates are also not tightly clustered around 2 Hz, even though the wind penetration is high.

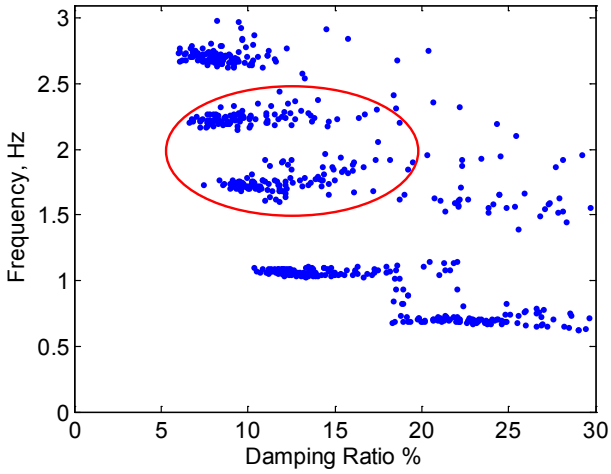

Figure 80. Modal frequency and damping estimates for high-wind conditions on October 7, 2011, from 8:00 to 10:00 UTC

In Figure 80, the wind power penetration was above 20% and the wind power is approximately 7,000 MW at 9:00 UTC. The figure shows that the frequency estimates (the spread across the y-axis) are more tightly clustered, but the damping estimates change throughout the 2-hour window of data. Another change is that the modal frequency has shifted so that there is no longer a 2-Hz mode, but instead two neighboring modes, located at 2.26 Hz and 1.74 Hz. Another example taken from the same day in Figure 81 shows modal estimates made during a new record for wind power when the wind power output reached 7,400 MW at 20:06 UTC. The modal frequencies during this

time of the day have changed so that now there is a modal frequency at 2 Hz. The mode is not as tightly clustered as it was in the examples from early 2009. The change in modal frequency and the spread of the damping as well as the tightness of the clustering of the modal estimates indicates that a lot of different variables besides wind power and wind penetration could have an effect on the modes present in the power system.

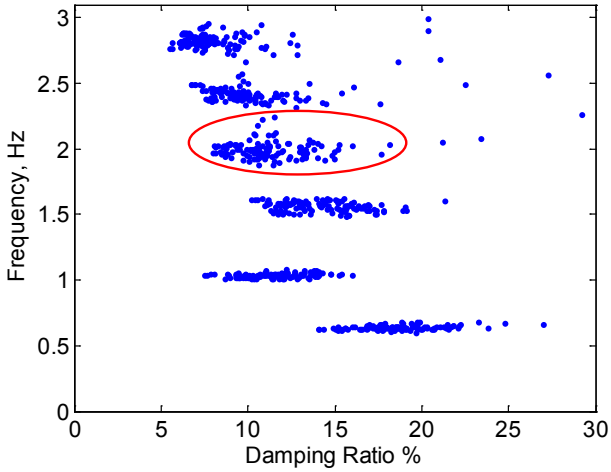

Figure 81. Modal frequency and damping estimates for high-wind conditions on October 7, 2011, from 19:00 to 21:00 UTC

A final example in Figure 82 is taken during a time when the wind power output of 3,000 MW, which is approximately the same as the wind power output during the April 13, 2009, case. However, here the wind power penetration is lower, at about 7% to 9%. Figure 82 shows the modal estimates from 00:00 to 02:00 UTC.

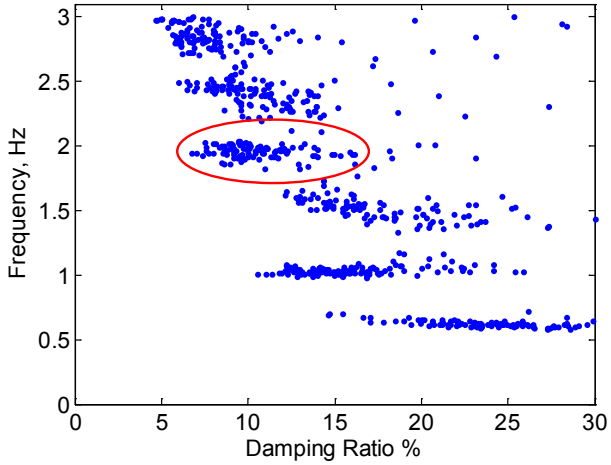

Figure 82. Modal frequency and damping estimates for high-wind conditions on November 1, 2011, from 00:00 to 02:00 UTC

A comparison of all the modes during high penetration levels is shown in Figure 83 to Figure 88. Each comparison is of a typical high-wind modal behavior in April 2009 to high-wind modal behavior examples from January 2010 to January 2012. When comparing the modal behavior, it is easier to see how the modes have changed over time.

In all cases, the spread along the x-axis is greater and shifted toward the right, meaning the modes are better damped. When the oscillations are better damped, damping estimates are more difficult to make because the oscillation in the signal has a shorter duration compared to a lightly damped oscillation. The frequency estimates also change, but these changes aren't consistent and even change throughout the day. For example, the modes shown in Figure 85 and Figure 86 are both taken from the same day but the frequencies are different. Early in the day, as shown in Figure 85, there is a frequency below 2 Hz, but later in the day, as shown in Figure 86, there is a frequency at almost exactly 2 Hz.

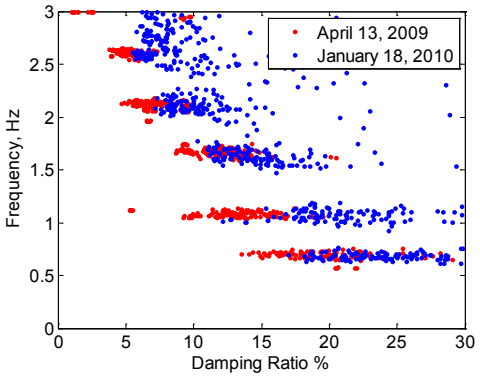

Figure 83. Comparison of modes during high-wind conditions in April 2009 and January 2010

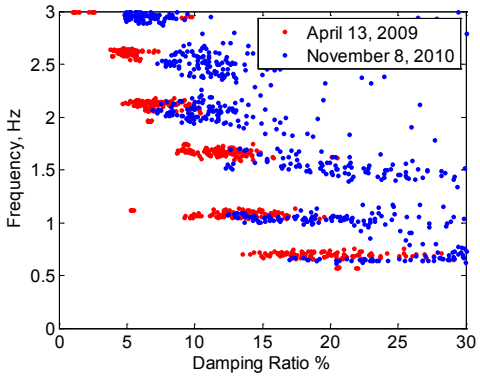

Figure 84. Comparison of modes during high-wind conditions in April 2009 and November 2010

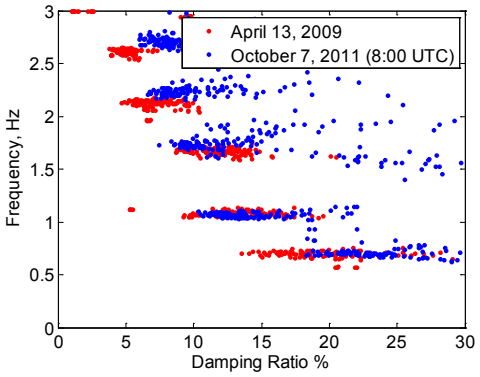

Figure 85. Comparison of modes during high-wind conditions in April 2009 and October 2011 (a)

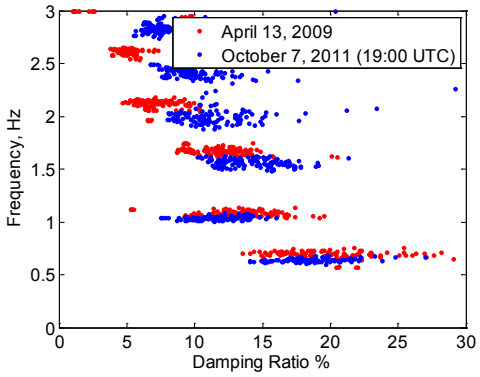

Figure 86. Comparison of modes during high-wind conditions in April 2009 and October 2011 (b)

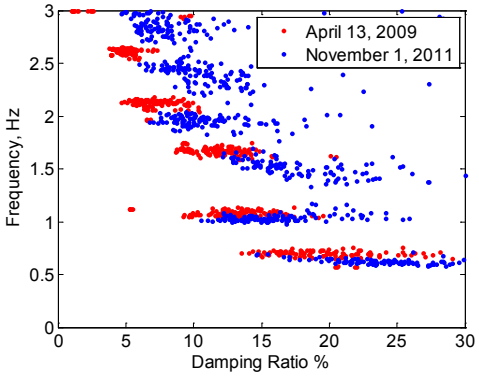

Figure 87. Comparison of modes during high-wind conditions in April 2009 and November 2011

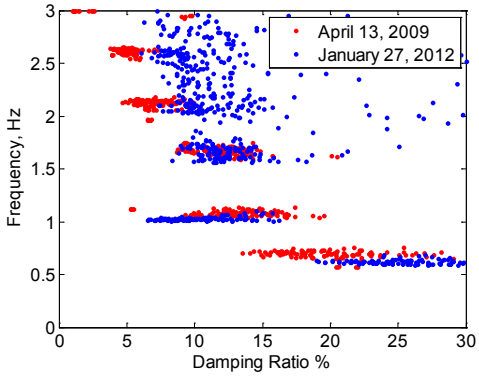

Figure 88. Comparison of modes during high-wind conditions in April 2009 and January 2012

These examples illustrate the power of PMUs to document changes in power system behavior over time. However, the data used to find the relationship between trends measured by PMUs and the wind power output for ERCOT is limited. At this time, it is not possible to make a conclusive statement about the effect wind power has on the power system as measured by PMUs. The ERCOT wind data is not always available, and is limited to less than two years of data taken at a rate of one sample per minute. ERCOT wind data is now only available in PDF format as hourly averages. The wind data used is aggregated wind power for all of ERCOT and does not take into account variation in output between wind resource regions. As more wind power plants are installed over a larger geographical area, it will become difficult to use the limited number of PMUs currently in the system to make accurate analysis on the effects of wind power on PMU measurements. As more PMUs are installed and more wind data becomes available, a more accurate analysis can be conducted, and PMUs will become a more valuable tool for tracking long term bulk power system behavior changes, particularly changes resulting from adoption of wind and other variable generation.

7 Conclusion

In this report, the algorithm used to screen PMU data generated by the UT-Austin synchrophasor network for power system events was described. The algorithm uses four different methods to screen for possible events. Each method is applied to a moving window of PMU data. The FFT and Yule-Walker methods are based on using the maximum magnitude of the spectral content of PMU signals to detect possible events. The matrix-pencil method is a parametric method that estimates parameters to fit the PMU signal. The two maximum amplitudes are used to screen for possible events. The min-max method screens for large fluctuations in the PMU data. Results from the four methods are collected for one hour of PMU data. Any values from each method that exceed three standard deviations away from the mean are marked as possible events. A data window is marked as containing an event if two or more methods detect a possible event in the same data window.

The algorithm was applied to 24 hours of PMU data to analyze how well the algorithm was able to detect large and small events. A large event caused by a sudden loss of generation was easily detected in both the UT-Austin and McDonald PMU frequencies and the voltage phase angle separation between the two PMU stations. Two smaller events were present in the PMU data as well. In the UT-Austin PMU frequency, a strong oscillation at approximately 1 Hz was visible but was not present in the McDonald PMU frequency. A reclosing event was detected in the McDonald PMU frequency and voltage phase angle. However, it is difficult to determine if the reclosing event was located on the distribution or transmission system. Once an event is detected by the algorithm, the data window containing the event is saved for further analysis.

The events detected from a screening algorithm are placed into categories based on common characteristics. First, the events are placed into categories based on visual inspection. These categories are impulse, transient, and step change for RPAD events and impulse, transient, and change in frequency for frequency events. The characteristics are extracted from each category and used to write an algorithm that automatically identifies events in PMU data.

8 References

[1] Allen, A.J.; Sang-Wook Sohn; Grady, W.M.; Santoso, S., "Validation of distribution level measurements for power system monitoring and low frequency oscillation analysis," *Power Electronics and Machines in Wind Applications (PEMWA), 2012 IEEE* , vol., no., pp.1,5, 16-18 July 2012

[2] Office of the Governor, Economic Development & Tourism. "Wind Energy Potential in Texas" and "Wind Farm Locations in Texas." Austin, TX: 2010. Accessed March 2012: http://governor.state.tx.us/ecodev/business_research/maproom/.

[3] Electric Reliability Council of Texas (ERCOT). Daily Grid Operations Reports. Austin, TX: 2004–2010. www.ercot.com/gridinfo/congestion/operations/.

[4] Kundur, P. *Power System Stability and Control.* New York: McGraw, 1994.

[5] Matlab Version 7.12.0. Natick, Massachusetts: The Mathworks Inc.

[6] Rogers, G. *Power System Oscillations.*New York: Springer, 1999.

[7] Liu, G.; Quintero, J.; Venkatasubramanian, V., "Oscillation Monitoring System Based on Wide-Area Synchrophasors in Power Systems." *Bulk Power System Dynamics and Control—VII. Revitalizing Operational Reliability, iREP Symposium*; 2007.

[8] Phadke, A.G.; Thorp, J.S. *Synchronized Phasor Measurements and Their Applications.* New York: Springer, 2008.

[9] Midwest Reliability Organization Protective Relay Subcommittee. *Considerations for Transmission Reclosing Practices in the MRO Area*. Roseville, MN: 2009. www.midwestreliability.org/03_reliability/studies_reports/transmission_reclosing_paper_090302.pdf.

[10] Allen, A.J.; Santoso, S.; Grady, W.M. "Voltage Phase Angle Variation in Relation to Wind Power." *IEEE Power and Energy Society General Meeting Proceedings*; July 25–29, 2010; pp.1–7.

[11] Grady, W.M.; Costello, D. "Implementation and Application of an Independent Texas Synchrophasor Network." *2010 63rd Annual Conference for Protective Relay Engineers Proceedings*; March 29, 2010–April 1, 2010; pp.1–12.

[12] Electric Reliability Council of Texas. *Report on Existing and Potential Electric System Constraints and Needs*. Taylor, TX: December 2010. www.ercot.com/content/news/presentations/2011/2010%20Constraints%20and%20Needs%20Report.pdf.

[13] Electric Reliability Council of Texas. *Report on Existing and Potential Electric System Constraints and Needs*. Taylor, TX: December 2011. www.ercot.com/content/news/presentations/2012/2011%20Constraints%20and%20Needs%20Report.pdf.

[14] Electric Reliability Council of Texas. *ERCOT Wind Integration Reports* Taylor, TX. www.ercot.com/gridinfo/generation/windintegration/.